**Universidade de Aveiro**

**2017**

Departamento de Engenharia de Materiais e Cerâmica

**Anna De Marzi**

# Fabricação aditiva de suportes 3D porosos de um vidro bioativo isento de alcalinos para aplicações médicas

Universidade de Aveiro Departamento de Engenharia de Materiais e Cerâmica
2017

Anna De Marzi

# Additive manufacturing of 3D porous alkali-free bioactive glass scaffolds for healthcare applications".

# Fabricação aditiva de suportes 3D porosos de um vidro bioativo isento de alcalinos para aplicações médicas

Tese apresentada à Universidade de Aveiro para cumprimento dos requisitos necessários à obtenção do grau de Mestre em Engenharia de Materiais, realizada sob a orientação científica do Doutor José Maria da Fonte Ferreira, Professor Associado com Agregação do Departamento de Engenharia de Materiais e Cerâmica, e do Doutor Hugo Alexandre Gonçalves da Rocha Fernandes, bolseiro de pós-doutoramento.

**Universidade de Aveiro**
**2017**

Departamento de Engenharia de Materiais e Cerâmica

**Anna De Marzi**

# Fabricação aditiva de suportes 3D porosos de um vidro bioativo isento de alcalinos para aplicações médicas

Tese apresentada à Universidade de Aveiro para cumprimento dos requisitos necessários à obtenção do grau de Mestre em Engenharia de Materiais, realizada sob a orientação científica do Doutor José Maria da Fonte Ferreira, Professor Associado com Agregação do Departamento de Engenharia de Materiais e Cerâmica, e do Doutor Hugo Alexandre Gonçalves da Rocha Fernandes, bolseiro de pós-doutoramento.

**o júri**

presidente **Prof. Doutor Augusto Luís Barros Lopes**

professor auxiliar do Departamento de Engenharia de Materiais e Cerâmica da Universidade de Aveiro

**Doutora Paula Alexandrina de Aguiar Pereira Marques**

equiparado a investigador Principal do Departamento de Engenharia Mecânica da Universidade de Aveiro

**Prof. Doutor José Maria da Fonte Ferreira**

professor associado do Departamento de Engenharia de Materiais e Cerâmica da Universidade de Aveiro

**agradecimentos**

I would like to firstly thank prof. José M. F. Ferreira for his availability and time dedicated to help me during my months in the Department of Material Engineering of the University of Aveiro. With him, my co-supervisor, Hugo Fernandes for all the assistance he offered and the great patience for my mistakes.

Moreover, I would like to thank all the colleagues present in the laboratory every day, for the support and the advices. Especially I thank Sofia, Bo and Inês for all the almoços and cafes spent together: a great distraction from the lab work. With them, I would like also to thank David, Ajay, Avito and Paula for all the help and availability showed.

At last, I thank my family. Sometimes it's easier to take all for granted, but this time here in Erasmus teach me how, without them, I would have not been the person I am today, good and bad way.

**palavras-chave** Engenharia de tecidos, vidro bioativo, robocasting, *scaffolds*.

**resumo**

A Engenharia de tecidos é um campo de estudo multidisciplinar baseado nas técnicas, métodos e conhecimentos derivados das áreas da biologia, medicina e engenharia. O objetivo é produzir dispositivos artificiais capazes de atuar como substitutos temporários de tecidos danificados: a estrutura obtida deve servir de suporte para a fixação e proliferação de células, bem como para a produção de matriz extracelular, idealmente até o mesmo dispositivo se degradar. Os grandes problemas relacionados a esta abordagem requerem a selecção adequada de um material e de uma técnica de processamento das estruturas de suporte.

Neste projeto de tese foi selecionada uma composição de vidro bioativo isento de álcalis no sistema binário de Diópsido - Fostato Tricálcico que já mostrou propriedades promissoras para engenharia de tecidos e regeneração óssea. A técnica de robocasting foi adotada para fabricação de andaimes porosos 3D com estruturas e porosidades projetadas por CAD e adequados para as funções almejadas.

O trabalho incluiu diferentes etapas, tais como: (i) preparação e caracterização de pós de vidro com diferentes distribuições granulométricas como forma de aumentar a capacidade de empacotamento; (ii) preparação de suspensões concentradas e estudo da dependência das suas propriedades reológicas do teor de sólidos e da quantidade adicionada de CMC, selecionado como único aditivo de processamento; (iii) produção dos *scaffolds* com diferentes porosidades; (iv) caracterização das estruturas impressas antes e após o processo de sinterização.

Os resultados obtidos demonstraram que uma mistura 1:1 de pós de vidro com diâmetros médios de partículas de 1 □m e de 4 a 5 □m permite a preparação de suspensões adequadas, alterando com o conteúdo de CMC e com a carga de sólidos. Os *scaffolds* impressos apresentam geometrias bem definidas e boa retenção da forma. O trabalho realizado pode ser considerado um ponto de partida muito interessante para estudos futuros com vista a obter melhorias adicionais.

**keywords** Tisuue Engineering, bioactive glass, robocasting, *scaffolds.*

**abstract**

Tissue Engineering is a multidisciplinary field of study based on the techniques, methods and knowledge of biology, medicine and engineering. The aim is to produce artificial devices able to act as temporary substitutes of damaged tissues: the structure realized must serve as supports for cell attachment and proliferation as well as the production of extracellular matrix, ideally until the same device degrades. The great issues related to this approach are therefore implementing a suitable scaffold material produced with an adequate technique in order to satisfy the above requirements.

In this Thesis project, an alkali-free bioactive glass composition in the binary system of Diopside-Tricalcium Phosphate that has already shown promising properties for tissue engineering and bone regeneration was selected. The robocasting technique was adopted for manufacturing 3D porous scaffolds with adequate structures and porosities designed by CAD.

The work included different steps such as: (i) preparation and characterization of glass powders with different particle size distributions to enhance the packing ability; (ii) preparation of concentrated suspensions and investigate the dependence of their rheological properties on solid loading and the content of CMC selected as the single processing additive; (iii) production of the scaffold with different porosity; (iv) characterization of the printed structures before and after sintering process.

The results obtained demonstrated that a 1:1 mixture of glass powders having mean particle diameters of 1 □m and 4–5 □m enables preparing suitable suspensions by playing with the contents of CMC and solid loading. The printed scaffolds present well-defined geometry and good shape retention. The work carried out could be considered as a very promising starting point for further studies aiming at obtaining further improvements.

# Index

Index ..... i

Index of Figure ..... iii

Index of Table ..... v

CHAPTER 1 ..... 1

Introduction ..... 1

1. Framework ..... 1

2. Objectives ..... 2

3. Thesis Organization ..... 3

CHAPTER 2 ..... 5

State of Art ..... 5

1. Bone tissue, injury and regeneration ..... 5

1.1. Structure of bone tissue ..... 5

1.2. Bone tissue growth ..... 7

1.3. Bone tissue injury and regeneration ..... 8

2. Current clinical approaches for bone repair ..... 8

2.1. Implantation ..... 9

2.2. Transplantation ..... 10

3. Bioengineering strategy ..... 10

3.1. Bioactive Glasses ..... 11

3.2. Bioactive glasses: previous researches and novelties ..... 13

4. Manufacturing method ..... 15

4.1. Robocasting ..... 16

4.1.1. Suspensions preparation and characterization ..... 18

4.1.1.1. Surface Proprieties ..... 18

CHAPTER 3 ..... 23
Experimental Procedure ..... 23
1. Glass composition, preparation and characterization ..... 23
2. Scaffold production and characterization ..... 28
2.1. Microstructure ..... 29
2.2. Pore Size ..... 29
2.3. Porosity ..... 30
2.4. Mechanical Strength ..... 31
CHAPTER 4 ..... 33
Results and Discussion ..... 33
1. Glass Characterization ..... 33
1.1. Crystallographic Analysis ..... 33
1.2. Size Reduction and Granulometric Analysis ..... 34
2. Paste Characterization ..... 36
3. Scaffold Characterization ..... 43
3.1. Morphologic Analysis ..... 43
3.2. Pore Size ..... 44
3.3. Porosity ..... 45
3.4. Mechanical Strength ..... 45
Conclusions ..... 49
Future Work ..... 50
Bibliography ..... 53

# Index of Figure

Figure 1. Internal structure of the bone. (68) ..... 6
Figure 2. Processing of remodelling of an injured bone. (54) ..... 8
Figure 3. Schematic representation of the double layer. (64) ..... 18
Figure 4. Potential curve derived by the sum of repulsive and attractive potential, as described by the DLVO theory. (66) ..... 20
Figure 5. CAD model of the scaffold printed with three different porosities: 300µm (a), 400µm (b), 500µm (c) ..... 28
Figure 6 . Illustration of the design parameters on the 3D scaffold ..... 29
Figure 7. XRD of the Di70-TCP30 bioactive glass, with amorphous structure. ..... 33
Figure 8. XRD of the Di70-TCP30 bioactive glass after sintering, with amorphous structure. ..... 34
Figure 8. Particle size distribution after different time of the bioactive glass in the planetary milling machine. ..... 35
Figure 9. Particle size distribution after different time of the bioactive glass in the attrition milling machine. ..... 36
Figure 10. Viscosity profile of suspension with increasing amount of solid loading and fixed quantity of CMC. ..... 37
Figure 11. Visco-elastic behaviour of suspension with increasing amount of solid loading and fixed quantity of CMC, analysed in the oscillatory mode. ..... 38
Figure 12. Effect of the increased amount of CMC with fixed solids loading. ..... 40
Figure 13. Viscosity profile of suspension with increasing amount of solid loading and variable quantity of CMC ..... 40
Figure 14. Visco-elastic behaviour of suspension with increasing amount of solid loading and variable quantity of CMC, analysed in the oscillatory mode. ..... 42
Figure 15. Magnification of printed scaffold before sintering with different porosity; (a) 300µm, (b) 400µm, (c) 500µm. ..... 43
Figure 16. Side section of printed scaffolds before sintering with different porosity; (a) 300µm, (b) 400µm, (c) 500µm. ..... 43

Figure 17. Side section of printed scaffolds after sintering with different porosity; (a) 300µm, (b) 400µm, (c) 500µm. ..... 44
Figure 18. Magnification of printed scaffold after sintering with different porosity after sintering; (a) 300µm, (b) 400µm, (c) 500µm. ..... 44
Figure 19. Tensions values of the samples with different pore size. ..... 46

# Index of Table

Table 1. Representation of the main advantages and disadvantages of the principal classes of biomaterials. ..... 12
Table 2. Weight percentage composition of the Di70-TCP30 bioactive glass. ..... 23
Table 3. Illustration of the different combination of Vol. % of solids and wt. % of CMC studied. ..... 27
Table 4. Design parameters for the scaffold production. ..... 28
Table 5. Average values of the sample dimensions and weight. ..... 30
Table 6. Pore sizes calculated from the SEM images and relative shrinkage in case of different porosity ..... 45
Table 7. Pore size and porosity values calculated. ..... 45
Table 8. Tension values of the samples, refered to the different pore sizes. ..... 46

# CHAPTER 1

# Introduction

In this chapter, a brief general introduction to the main aspects of this Thesis is made, including the motivations behind the proposal, stating the overall objectives we intend to achieve, and experimental approach we want to test. The general organization of this Thesis will be also exposed.

## 1. Framework

The life expectancy has been increased in the last centuries, mainly cause of the improvement of medicine and researches around medical innovations. On the other hand, the rise of life span has led to deal with the population ageing and, consequently, the diseases associated to it, such as osteoarthritis and osteoporosis (1). These conditions of the musculoskeletal system imply the loss of continuity and strength of the bone section and are mainly caused by the lack of nutritional, pathologic or metabolic factors, mostly associated with the increasing of sedentary life. This deficiency leads to an imbalance between the cells which work on the bone tissue: osteoblasts that contribute to the tissue formation, and osteoclasts, which permit bone reabsorption. When the activity of osteoclasts prevails over that of osteoblasts the bone starts to degrade (2).

To overcome those bone diseases many improvements were made along the last decades aiming at developing new bone regeneration strategies and especially by combining bioengineering technologies and methods with medicine in the field of tissue repair (3).

This solution presented is associated with the tissue engineering, an interdisciplinary field that applies the knowledge of engineering, biology and chemistry in solving the critical medical problems of tissue loss and organ failure. The great issue related to this work is the

manufacturing of a device suitable to bone tissue repair, thus enabling regeneration, especially from the functionality recovery perspective.

From this point of view, it must be ensured not only a certain internal structure (*interconnected porosity*) but also specific chemical properties that enable scaffold material to promote tissue regeneration (4). As such, the material should meet a set of important requirements: must be biocompatible and bioactive to facilitate cells colonization and have an adequate interaction with human body, to avoid the attack of the immunity system, but also shows adequate mechanical properties to support the load during recovery. Nowadays many materials can be used for scaffold, either naturals or synthetics: in the field of bone tissue repair, bioactive glasses show promising characteristics, thanks to the high interfacial bonding and response as they interact with body fluids (5).

Choosing the material is not the only main issue; the processing technique is also important since it will directly affect the final properties, mechanical and especially structural, of the scaffold. From this perspective, there are numerous processing techniques to produce bioactive glass scaffolds. Best results have been obtained with *Solid Freeform Fabrication* (SFF) instead of conventional production methods, because it allows a high control of the printed structure. However, this kind of technique is based on the creation of a stable suspension: the analysis and control of its rheological properties is fundamental in order to be able to extrude the paste and to obtain at the end, a scaffold with precise geometry.

## 2. Objectives

The aim of this Thesis is to produce scaffold for bone tissue regeneration by using an alkali-free bioactive glass with robocasting technology: the association of both these requests represent a novelty in this field of research. In fact, the most well-known is the alkali-containing 45S5 Bioglass®, which has been implemented many times in tissue engineering but presents several problems that derive mostly from its high sodium content (6). The leaching of sodium and the consequent ionic exchange with hydrogen ions results in suspensions with high pH values, making the processing in aqueous environment very difficult (7).

To overcome these problems, an alkali-free bioactive glass composition was selected consisting of 70 *Diopside* (Di) and 30 *Tricalcium Phosphate* (TCP) (wt.%), corresponding to (mol%): 36.52 $CaO$ – 19.24 $MgO$ – 38.48 $SiO_2$– 5.76 $P_2O_5$ (8). The easiness of processing is expected

to enable the fabrication of porous 3D structures with well-defined pore sizes (both *micro* and *macro*) and interconnectivities. The absence of alkaline oxides is expected to enhance the easiness of colloidal processing in aqueous media and obtain suspension with high solid loadings and rheological properties suitable for additive manufacturing by the robocasting process.

This study should be considered as a preliminary research about if the merge of these two technologies (the alkali-free bioactive glass and the robocasting). Both of them have already been studied and implemented in different systems: their union should be, not only promising from the theoretical point of view, but also from the practical one.

## 3. Thesis Organization

This Thesis work will be divided in different parts. This first Chapter provides a general introduction to the topic, states the motivations behind it, announces the main intended objectives, highlights the novelty aspects, and gives account about the experimental approach that will be followed along the study. Chapter 2 reviews the state of the art in this area and highlights the aspects that still need to be improved, thus justifying the undertaking of this work. Chapter 3 will describe all the aspects related to experimental procedures adopted along the Thesis. Chapter 4 will present the results obtained and the related discussion. The main conclusions will be presented in Chapter 5, while any future issues worthy to be further investigated in the future will be pointed out in in Chapter 6.

# CHAPTER 2

# State of Art

This Chapter presents an updated overview about the state of art on this field of research, including the main issues related to bone tissue injury and regeneration, as well as how bioglass composition affects its degradation, bioactivity, thermal properties and processing ability.

## 1. Bone tissue, injury and regeneration

### *1.1. Structure of bone tissue*

Human skeletal system is the internal skeleton that serves as a framework for the body. This framework consists of many individual bones, cartilages and bands of fibrous connective tissue—the ligaments and the tendons—in intimate relationship with the parts of the skeleton (9).

The functions of the skeleton are of three different types: support, protection, and motion. The great majority of the skeletal muscles are firmly anchored to the skeleton, usually to at least two bones and in some cases to many bones. Thus, the motions of the body and its parts, all the way from the lunge of the football player to the delicate manipulations of a handicraft artist or of the use of complicated instruments by a scientist, are made possible by separate and individual engineering arrangements between muscle and bone (10).

Bones are divided into four basic types based on the shape of the bone: they can be long, short, flat or irregular. Long bones are longer than they are wide and are primarily found in the appendages (arms and legs). They include the femur, tibia, fibula, radius, ulna, and humerus. Long bones are slightly curved for strength and designed to absorb stress at several points. Short bones are basically cube shaped and are about as wide as they are long. Examples are the bones found in the wrist and ankle. Flat bones are thin and generally flat.

They offer considerable protection and a great deal of surface area for muscles to attach. Examples of flat bones are the cranial bones, which protect the brain, and the scapula (shoulder blade). Irregular bones include many of the bones that do not fall into the other three categories. They have complex shapes and include bones like the vertebrae (11).

Bone tissue can be described as a hard and consistent organ which composes the skeleton of vertebrates and considered as a mineralized connective tissue formed by cells, that deposit a matrix of collagen and release *Ca*, *Mg* and $PO_4^{3-}$ ions which combine with the matrix to form a "bone mineral" (hard and flexible). There are two type of bone tissue: *cortical*, composes the compact and hard zone of the bone (external), and *cancellous*, the spongy internal structure of the bone.

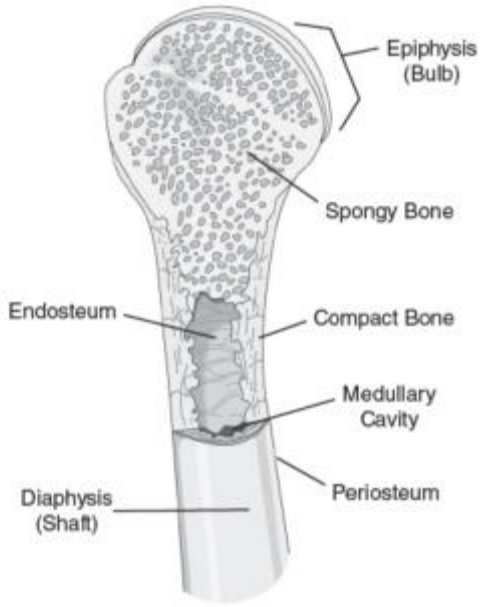


***Figure 1. Internal structure of the bone. (68)***

Their structures imply that the two types differ in density, or how tightly the tissue is packed together. The lighter type (cancellous) is in the internal zone of the bone, while the compact one (cortical) composes the external part, as it's showed in Figure 1. The spongy bone is less dense and contains spaces so blood vessels and other nutrients can be supplied to the bone. The compact part of the bone contains few spaces and provides protection and strength. The differences of structure and functions between these parts of the bone lead also to different mechanical behaviour: it's been researched that the density of the bone directly affect its stiffness and its response to external loadings and forces. From this point of view, even if both made of the same material, the spongy part tends to present a Young's Modulus

value ten times less than the compact one, since it's around 1GPa, while the other is about 17GPa (12) (13) (14) (15).

Bone contains a relatively small number of cells entrenched in a matrix of collagen fibers that provide a surface for inorganic salt crystals to adhere. These salt crystals form when calcium phosphate and calcium carbonate combine to create hydroxyapatite, which incorporates other inorganic salts like magnesium hydroxide, fluoride, and sulphate as it crystallizes, or calcifies, on the collagen fibers. The hydroxyapatite crystals give bones their hardness and strength, while the collagen fibers give them flexibility so that they are not brittle. Although bone cells compose a small amount of the bone volume, they are crucial to the function of bones. There are different types of cells that contribute to bone homeostasis: osteoblasts, osteoclasts and osteocytes (16). The most important are osteoblasts, which are bone-forming cell, and osteoclasts which can resorb or break down bone. The equilibrium between these cells maintains the bone tissue in its healthy form. (17)

## *1.2. Bone tissue growth*

The skeleton of the human body starts to form in the fourth month of pregnancy, together with cartilage and connective tissue. This process is known as ossification, and it specifically indicates the natural process of bone formation, which could be simplified to the process of proliferation of mesenchymal cells which later condense into compact nodules. Some of these cells develop into osteoblasts, which secrete a collagen-proteoglycan matrix that is able to bind calcium salts. Through this binding, the prebone (osteoid) matrix becomes calcified. (18) In most cases, osteoblasts are separated from the region of calcification by a layer of the osteoid matrix they secrete. Occasionally, osteoblasts become trapped in the calcified matrix and become osteocytes—bone cells. The entire region of calcified spicules becomes surrounded by compact mesenchymal cells that form the periosteum (a membrane that surrounds the bone). The cells on the inner surface of the periosteum also become osteoblasts and deposit osteoid matrix parallel to that of the existing spicules. In this manner, many layers of bone are formed.

Bone development continues also throughout adulthood enduring the repair of fractures and the remodelling the bone structure (19): it can be simplified to a matrix resorption from one to another bone surface (injuries, exercise and other activities lead to this process) (9).

### 1.3. Bone tissue injury and regeneration

The injury of bone tissue can be caused by different events like trauma, cancer and aging. Generally, all these events lead to the loss of continuity of the bone structure or its inflammation and degradation.

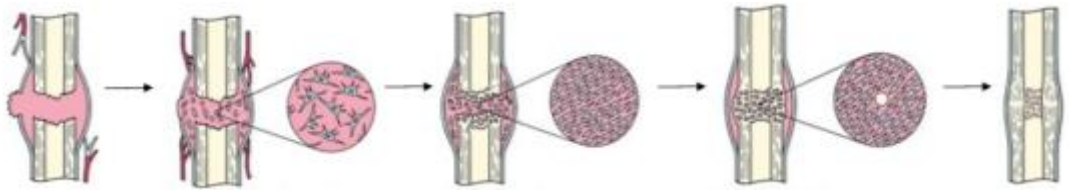

***Figure 2. Processing of remodelling of an injured bone. (54)***

The bone remodelling process is under the control of local (i.e., growth factors and cytokines) and systemic (i.e., calcitonin and oestrogens) factors that all together contribute to bone homeostasis. Bone metabolism relies on complex signalling pathways and control mechanisms to achieve proper rates of growth and differentiation. These controls include the action of several hormones.

The remodelling cycle of bone tissue consists of three consecutive phases, as shown in Figure 2: resorption, during which osteoclasts digest old bone; reversal, when mononuclear cells appear on the bone surface; and formation, when osteoblasts lay down new bone until the resorbed bone is completely replaced. An imbalance between bone resorption and formation can result in bone diseases including osteoporosis.

The regeneration of bone tissue is possible and is conducted by the process of tissue calcification, but this procedure is not always permitted (due to the site of the fracture, i.e. dental bone, where tissue regeneration cannot take place naturally, but may need the implantation of some devices or stem cells (20)) or the best solution (because i.e. it can lead to the stiffening of bones that are usually flexible).

## 2. Current clinical approaches for bone repair

Current clinical procedures that involve the repair of bone defects include implantation or transplantation.

## *2.1. Implantation*

It's possible to classify an implant as any external artificial device which will be inserted in the human body in order to recover a failed tissue or biological structure. Implants can be made out from different materials, both bioinert, such as titanium or silicone, which are chemically stable but tend to have minimal interactions with the human body, both biodegradable and bioabsorbable, such as lactic acid copolymers and bioglasses (21).

It's necessary to underline, however, how these last types of materials were implemented only in recent times (some specific application is reported from literature (22) (23)), while, bioinert materials were the first type of implants used as tissue recovers.

The problems of this first approach involving bioinert artificial implants are their lack of self-repair, blood supply and structural adaptation to external factors, such as mechanical load. The contact between body internal apparatus, the immune system and the inert synthetic material might also bring some complications (24).

Is it known that no material is completely inert when in the biological environment. When inertness prevails, the material lives as a host trying to support the injured tissue but also interact with the external environment and suffers from the immune attack. This leads to the negative response of the body organism, which also depends on the composition, morphologic and geometric characteristics of the surface.

Many attempts have been made (25) to create artificial implants with an appropriate outside layer or different composition (26) but this solution only evaluates the mechanical properties (27) and osteointegration (28).

Lack of self-repair, blood supply and adaptation to external factors are other characteristics of the artificial implantation method. The issue with those is that, even if it is inert, the material installed is not everlasting and needs to be replaced after 10-15 years, due to the wear and stresses it undergoes during its life (29).

### 2.2. Transplantation

Transplantation is defined in surgery as the act to transfer an organ (i.e. hearth, kidneys, liver) or a tissue (i.e. bones, tendons, cornea) from one part of the body, of one person, to another. Here there is no problem about the inert behaviour of the bone repair device, because it is a natural material which will interact with the body environment and structures as it already did.

This type of method is not lack of shortcomings, which include the long waiting list, the little number of compatible donors and the risk of rejection or infection.

In both cases, artificial or prosthetic materials for replacing limbs, teeth, and other tissues resulted in the partial restoration of lost function and not its complete recovery of their natural activity.

## 3. Bioengineering strategy

Bioengineering can be described as an interdisciplinary application of two main sciences, engineering and medicine: the aim of this merge is to fill the gap between methods, technologies of mechanics, and the understanding of the human body.

Tissue engineering is a segment of this study that applies the knowledge of bioengineering in solving the critical medical problems of tissue loss and organ failure. Tissue engineering has been formally defined as “the application of the principles and methods of engineering and the life sciences to the fundamental understanding of structure–function relationships in normal and pathological mammalian tissues and the development of biological substitutes that restore, maintain, or improve tissue function”. The idea is to produce a scaffold, made by different kind of materials, suitable for tissue cells colonization and its subsequent growth. This is possible by the harvesting of stem cells from the patient, which are then cultured on the scaffold that can be implanted after (30). What tissue engineering is trying to accomplish is to replace synthetic implants and tissue grafts, already being used in medicine, with the bioengineering approach that uses porous material scaffolds integrated with biological cells or molecules to regenerate tissues. Therefore, this new paradigm requires scaffolds that balance temporary mechanical function with mass transport to aid biological delivery and tissue regeneration in three dimensions. The synthetic scaffold, being used, should be as short lived as possible; at the same time the scaffold must maintain its

viability and integrity long enough for the cells to produce their own extracellular matrix (30) (31).

Tissue engineering can now rely on numerous research projects and papers which attest the benefits this science field can bring to tissues repair.

Primarily, it is based on nature imitation: this overcomes the main problem of transplantation, which is the shortage of donor tissue and organs and their compatibility with the patient body (32). Moreover, materials used to produce scaffolds are often biodegradable or bioabsorbable and this leads to the non-inert behaviour of the created structure and its complete interaction with human body environment. Designed material should not act just as a static replacement of the injured tissue but must can cause a cellular response: the scaffold implanted will degrade under immune system attack, with a certain rate, to allow colonization and cells growth, and to leave behind the renewed tissue (33).

## *3.1. Bioactive Glasses*

As mentioned in previous sections, scaffolds can be made out from different biodegradable or bioabsorbable materials: their composition and internal structure will affect their behaviour when in contact with biological environment. The idea is to create a solid capable of connecting to living tissues, and so able to allow cells colonization, but also capable to degrade. Generally, this type of materials has been formally defined as biomaterials.

A biomaterial is now defined as a substance that has been engineered to take a form which, alone or as part of a complex system, is used to direct, by control of interactions with components of living systems, the course of any therapeutic or diagnostic procedure. It can formally be defined as any matter, surface, or construct that interacts with living systems.

Today, materials used for scaffolds are natural or synthetic polymers such as polysaccharides, poly (a-hydroxyester), hydrogels or thermoplastic elastomers. Other important categories of materials are bioactive ceramics such as calcium phosphates and bioactive glasses or glass-ceramics. Specifically, those types of materials have a high interfacial bonding and response when in contact with internal body tissue.

***Table 1. Representation of the main advantages and disadvantages of the principal classes of biomaterials.***

| *Biomaterial* | *Advantages* | *Disadvantages* |
|---|---|---|
| *Polymer* | Composition flexibility, film and gel form | Weak, low mechanical properties |
| *Metal* | High strength, ductility, wear resistance | Low biocompatibility, corrosion, metal ions release |
| *Composite* | High elastic strength, low modulus, absence of corrosion | Short-term durability |
| *Ceramic/Glass* | Biocompatible, compression and corrosion resistance | Brittle, low fracture strength, high density |

As mentioned, the idea of bioengineering is to create a scaffold, or surface, able to imitate the functions and resistance properties of the tissue to recover. The choice of the material is a fundamental: this should both ensure mechanical assistance and to provide a suitable surface for cells to adhere, colonize and differentiate in order to promote the tissue regeneration. The biocompatibility, by this perspective, is one of the most attractive glass ceramics' properties, even if, as mentioned in the scheme (Table 1) above, those materials are characterised by brittle structure and high density. In fact, glass ceramics in general present adequate strength and interaction with living matter; especially, they tend to form a layer of hydroxyapatite (HA) on their surface: this mineral makes bioglass an active material. This means that it is osteoconductive, so able to serve as a scaffold for viable bone healing and permit infiltration of osteogenic precursor cells, and able to promote osteogenesis, which is the ability of the graft to produce new bone. bioglass is also osteoinductive: it is equipped to induce stem cells to differentiate into mature bone cells (34). This process is typically associated with the presence of bone growth factors within the graft material.

The main issue is now the production of a scaffold with a certain structure and made by bioactive glass. Only the correct combination of these factors can output a product able to permit bone tissue regeneration; correct pores size, vascularization, cells diffusion, and mechanical properties strictly depend on glass composition and how the scaffold is manufactured. Another important feature of biomaterials in general, is their ability to degrade under the attack of the immune system. This means that the material will dissolve in fragments and permit also the leaching of the ions which compose the scaffold: from this perspective, a lot of researches around biomaterials concerned how the elements of the choose material could affect both tissue regeneration and body response to the external device.

## *3.2. Bioactive glasses: previous researches and novelties*

The first bioactive glass was developed in 1970 by Larry Hench and colleagues. This bioactive glass composition consists of (in wt.%) 45% $SiO_2$, 24.5% $Na_2O$, 24.5% $CaO$, 6% $P_2O_5$, and is designated as 45S5 Bioglass® (35). This combination has been selected by the authors to provide a large amount of CaO with some $P_2O_5$ in a $Na_2O$ -$SiO_2$ matrix and is very close to a ternary eutectic, making it easy to melt (6). It entered clinical applications in 1985 and since then it has been widely used in dentistry, orthopaedics and maxillofacial surgery (36).

However, it is not considered to be the ideal biomaterial for inducing bone regeneration (37). One of the biggest problems attributed to the 45S5 Bioglass® relates to its high dissolution and degradation rates in vitro and in vivo (38) (39). An in vitro study using osteoblastic cells in the presence of glasses containing smaller amounts of sodium revealed that the sudden release of alkali ions caused a cytotoxic effect and decreased cell viability in comparison to an alkali-free composition (38). From this point of view, the 45S5 Bioglass® has a high dissolution rate (40). Consequently, this implicates a fast reabsorption which can negatively affect the natural bone remodelling and angiogenesis: the process of tissue repair is quicken, preventing its complete and uniform recovery, which can lead to the formation of a brittle bone. Specifically, the fast degradation rate of 45S5 Bioglass®, associated with its high alkaline content, does not suitably match the new bone growth rate leading to gap formation between the implant and bone tissue as concluded by Vogel et al. (41). Furthermore, Filho

et al. (42) observed that the development of a crystalline phase, $Na_2Ca_2Si_3O_9$, slightly reduced the rate of surface hydroxyapatite formation relative to amorphous bioactive glass 45S5. The above issue was partly solved by Clupper and Hench (42), who carried out quantitative investigations on the effect of crystallinity on the apatite formation on bioglass surfaces in vitro. Their findings revealed that the crystal phase $Na_2Ca_2Si_3O_9$ slightly decreased the formation kinetics of an apatite layer on the bioglass sample surface but it did not totally suppress the formation of such layer.

All the above referred shortcomings derived from the high sodium also makes the processing in aqueous environment very difficult due to the leaching of $Na^+$ ions during degradation of the scaffold and the consequent variation of the pH value: this could inhibit osteoblasts activity and promote cells necrosis (7) (43). Moreover, scaffolds or powder compacts made of 45S5 Bioglass® can hardly be sintered due to the proximity between the onset of crystallization temperature (Tc) and the glass transformation temperature (Tg), as has been extensively documented in several literature reports. Specifically, given the low Tc–Tg value, the printed scaffold is therefore likely fully crystalline prior to undergoing significant densification (T > 800 °C), and this behaviour leads bioglass to rapidly crystalize (44). As previously noticed, greater the crystalline phase and more will be the inert character of the bioactive glass and the less will be the densification. This would imply a more fragile scaffold that will be composed of particles weakly bonded together. Hence, a different and improved sintering protocol had to be implemented, to allow the production of a bioactive and biodegradable scaffold, with specific mechanical properties able to withstand the requirements for bone tissue regeneration.

Other problems with alkali-containing glasses are related to the manufacturing: higher the alkali oxides content and lower will be the working range (temperature interval for glass formation) and more difficult will be the wet processing (to create a suspension for additive manufacturing). Specifically, the optimal sintering temperature is close to the crystallization one: this lead to the devitrification of the system, because of the high crystalline phase, which promotes high mechanical properties and could favour a more inert behaviour. Bioactivity however, as already discuss, depends also on the chemical composition of bioglass: changing on the alkali content of the scaffold allows a more versatility behaviour of the crystallization and sintering temperatures.

Attempting to overcome the above referred drawbacks, a series of alkali-free bioactive glasses compositions were recently proposed. They were designed in the glass forming region of *Diopside* ($Di - CaMgSi_2O_6$) – *Fluorapatite* ($FA - Ca_5(PO_4)_3F$) – *Tricalcium phosphate* ($TCP - 3CaOP_2O_5$) ternary system (12), or in the binary ($Di - CaMgSi_2O_6$) – *Tricalcium phosphate* ($TCP - 3CaOP_2O_5$) system (8). The production of Tricalcium phosphate based scaffold has already been done to realise artificial bones (45). However, their low toughness make them not suitable for bone tissue regeneration: from this point of view, a Di-TCP system shows a higher ability to support heavy loading. Moreover, this composition lead to the formation of a glass with high bioactivity (39) cause of the higher number of $Q^2$ (Si) species (referring to the number of bridging oxygen atoms on the silica tetrahedon) and, thanks to the TCP, also with a good dissolution rate (8).

In this regard, the composition Di-70-TCP-30 (Di-70) revealed to be very promising, justifying its selection in the frame of this work. In this project the alkali-free bioactive glass (Di-70) will be used. The focus will be put on the production of scaffolds for medical purposes.

## 4. Manufacturing method

For the realization of a porous 3D structures with well-defined pore sizes and interconnectivities, in order to allow cell colonization and subsequent bone tissue regeneration, it's strictly related to the production technique: it affects costs, reproducibility and the preservation of raw material's properties.

In order to be certain that all the requests of the scaffolds are satisfied, it is necessary to choose the right manufacturing method that obey to the following principles:

- It must negatively the proprieties of the material shaped, neither both its chemical characteristics and bioactivity
- It must allow to produce a scaffold that in the end present the correct porosity and structure designed in the 3D CAD model
- It must be characterized by a solid reproducibility and easy scaffold designation

Nowadays there are numerous processing techniques that allow the creation of a porous scaffold with adequate mechanical properties and ions and cells diffusion inside it. The most

conventional and used ones, as solvent casting, particulate leaching, phase separation, cannot be implemented in this project. The main reason behind this statement is that these techniques require the use of a specific and complex molds, don't allow the precise control of the selected porosity and geometry, and, consequently the satisfaction of minimum mechanical proprieties. Moreover, these manufacturing methods cannot be easily used with bioactive glass or ceramics scaffolds in general.

## 4.1. Robocasting

It's necessary to investigate in other new technologies that allow the fabrication of materials with flexible processes. Best results have been obtained with Solid Freeform Fabrication (SFF) instead of conventional production methods: based on CAD models, it is possible to produce both simple and very complex scaffolds, in order to precisely recreate the part of bone to recover. Moreover, these techniques allow to control the porosity structure of the scaffold to facilitate cells and ions diffusion. In fact, a mandatory requirement for a scaffold, and particularly in bone engineering, is a controllable interconnected porosity to direct the cells to grow into the desired physical form and to support vascularization of the ingrown tissue.

Robocasting is an extrusion-based, direct writing technique that utilizes high solids loaded paste-like suspensions (*inks*) to build 3D structures through a layer-wise deposition of extruded cylinders from a CAD program. Among other methods, this one can provide all the ideal characteristics required for a scaffold for medical application needs.

However, additive manufacturing processes based on the deposition of a colloidal suspension that has been transformed into a pasty like system are very challenging in terms of rheological properties. They should not clog fine nozzles during the extrusion process and the extruded cylinders should be able to retain their shape right after deposition. These key requirements are hardly achievable when 45S5 Bioglass® is used. This explains why among a few thousands of papers about 45S5 Bioglass®, published up to 2013, there was not even one dealing with additive manufacturing. Only in this year a simple recipe was using carboxymethylcellulose (CMC) as single processing additive was for the first time used for the fabrication of porous 45S5 Bioglass® scaffolds by robocasting (7). From this point of view, challenging will be the creation of a suitable "ink": robocasting requires a suspension

with pseudo plastic behaviour and adequate stiffness (elastic modulus, G'), in order that it will shear thin and flow through the extruding orifice, but also maintain its shape. The realization of a dispersed high-solid-loading suspension of ceramic powder in a water medium is not yet functional to be implemented in this specific SFF technique, as it doesn't possess any yield stress. This parameter covers an important role since determines the viscous behaviour of the paste, over its elasticity: the slurry will flow only if a certain pressure is applied. This means that the rheology of the paste must be altered in order to create a partially flocculated suspension where a loosely bound particle network is formed. (46) From this perspective, as will be mentioned in the next Chapter, to obtain a paste with the above-mentioned characteristics is necessary to play whit particles surface properties of the material in the suspension.

From the robocasting point of view, to achieve this goal, the suspension is created by the dispersion of the ceramic powder in water, with the addiction of an anionic dispersant compound. These, according to the traditional approach, should be adsorbed on the particles surface and stabilize the suspension. After this, suitable concentrations of salts or cationic species are added in order to create a flowable slurry: their role is to provoke a rheological change of the system in order to obtain a paste-like system with adequate elastic properties. The use of many components in this system leads to a difficult balance between the forces present into it: generally anionic and cationic substances tend to change the pH of the suspension and consequently the non-stabilization of the system (47).

From this perspective, a simplified approach can be made by the using of a unique additive, the carboxymethylcellulose (CMC), which acts as multifunctional additive (binder, dispersant and gelation agent). Its low anionic behaviour facilitates adsorption and the versatility of rheological properties of the suspension, related to the MW added into it, and enables varying its flow properties. Specifically, CMC is a compound made of polymeric chains: they will interact with particles surface and partially being adsorbed into them. The remaining part of the polymer will adopt an extended configuration protruding from the surface, into the solution. The repulsion forces required for the creation of a partially flocculated suspension will arise from the compression mechanism between polymeric chains (48).

The key of this project is not only the material (bioactive, biodegradable, specific rheology) but also its geometry: robocasting procedure enables to produce scaffolds with customized

external structure (ability to adapt at the case of the patient) and internal pore architecture (to provide and facilitate bone tissue cells colonization).

The combination of robocasting printing method, on one side, and alkali-free bioactive glass, on the other, considering all the advantages discussed in the previous pages, will provide a solid alternative for the manufacturing of scaffold for bone tissue regeneration.

### 4.1.1. Suspensions preparation and characterization

As stated in the previous Chapter, the main purpose of this Thesis project is to evaluate the possibility of merging a material, an alkali-free bioactive glass, which showed promising properties in the field of tissue recovery, with a technique, the robocasting method, which exhibit favourable characteristics, in terms of geometry control. From this point of view the great issue encountered during the experimental work, was to create a glass dispersion suitable for the deposition and fabrication of a porous scaffold.

#### *4.1.1.1. Surface Proprieties*

A suspension can be generally defined as a dispersed phase of a two-component system in which the elements of the dispersed phase cannot be easily distinguished without the use of a microscope. Particles tend to interact with each other in different ways, depending on the particles surface characteristics and the additives used: these parameters promote the generation of forces which affect the aggregation degree of the system.

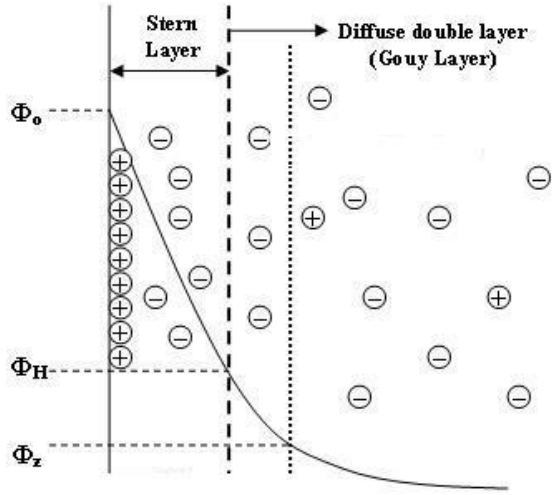


***Figure 3. Schematic representation of the double layer. (64)***

Colloidal particles, by virtue of their small size, have a very large specific surface area and consequently affect and promote adsorption. Suspending particles in a liquid lead to charging of the surface, by either surface acids or bases (such as carboxylic, silane, or sulphate groups), by adsorption of free ions, as is typical in clays, or by adsorption of surfactants or polyelectrolytes. From this perspective, unless any precautions are taken, colloidal particles generally carry an electrical charge. The presence of charged particles surfaces, as result of the superficial ionization/hydration and/or of the specific adsorption of charged species, affects the ions distribution in its surroundings. In particular, the counter-ions distribution around the charged particle surface can be described with the *double electric layer* theory. In the surroundings of the charged particle a layer of counter-ions, called *Stern layer*, will form; here, ions are strictly attached to the surface and the electric potential decreases linearly with the increasing of the distance. Beside this layer, another one, called *Gouy layer* and made of ions and counter-ions diffusion will take place: the potential here decreases exponentially (13).

The potential tends to be stable in the Stern region and, beyond it, decrease linearly under a constant, known as the *Debye length*, $k^{-1}$, which characterise the screaming effect produced by ions, as shown in the Equation 1:

$$k^{-1} = \sqrt{\frac{\varepsilon_r \varepsilon_0 k_B T \, e^2 \sum c_i z_i^2}{2 N_A e^2 I}} \tag{1}$$

where

$I$ is the ionic strength of the electrolyte (mole/m$^3$),
$\varepsilon_0$ is the permittivity of free space (farads per metre),
$\varepsilon_r$ is the dielectric constant (-),
$k_B$ is the Boltzmann constant ($1.3806\times10^{-23}$ J/K),
$T$ is the absolute temperature (K),
$N_A$ is the Avogadro number ($6.022\times10^{23}$ mol$^{-1}$),
$e$ is the elementary charge ($1.602\times10^{-19}$ coulombs).

The interaction potential influences the electrostatic forces between the particles. These forces depend interparticle' distance: lower the gap among them higher will be the magnitude of the interaction forces. Consequently, the amount of work required to aggregate

two charged particles depends on their electric potential: when this distance is high, the repulsion potential extends from the particle leading to a difficult aggregation and therefore to a stable suspension of dispersed particles.

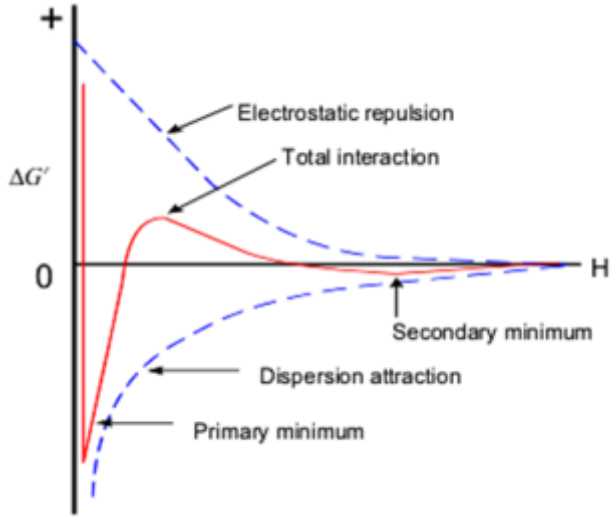


***Figure 4. Potential curve derived by the sum of repulsive and attractive potential, as described by the DLVO theory. (66)***

This process of stabilization by electrostatic repulsion is described by the DLVO theory (named after Boris Derjaguin and Lev Landau, Evert Verwey and Theodoor Overbeek), which sums the forces of attraction of Van der Waals and of repulsion of the double electric layer, in a unique potential function, illustrated in *Figure 4*. As showed, the curve of *total interaction* present a deep *primary minimum* and a *secondary minimum*, separated by an *energy barrier*, the maximum curve peak: this means that, to reach the aggregation point, particles must be close enough to enter in the *primary minimum* zone.

The stabilization of the suspension does not depend only on the distance between particles, but it's affected also by ions concentration and global charge, which influence the Debye length. On the other hand, the creation of a balanced suspension made out just from these parameters, can be only considered as kinetically stable: thermal fluctuations will eventually give enough energy to the particles to drive them over the primary minimum and allow aggregation. From this point of view, a more stable dispersed system can be achieved by ensuring a thermodynamic stability that can be imparted by steric repulsions from grafted or adsorbed active agents, known as dispersants. Those components stabilize ceramics suspensions by altering the natural condition and charge properties of the particle surface; their stabilization efficiency relays on the mechanism that create the repulsion forces

between particles. Generally, most known dispersants are polymeric molecules, with ionizable groups in the chains, which can easily connect to the particles and allow physical repulsion: a part of the polymer will adsorb and stick to the surface, while the rest will stretch and permit particles separation.

In other to realize a stable and dispersed suspension and simultaneously a paste able to be extruded, *carboxymethylcellulose* (CMC) was the selected as unique and multifunctional processing additive.

# CHAPTER 3

# Experimental Procedure

In this Chapter the experimental procedure will be presented, including the bioglass powder composition and preparation, as well as the main issues related to the manufacturing of a stable dispersion, able to be consequently printed with robocasting machine. Characterization of glass powder and suspension will be explained.

## 1. Glass composition, preparation and characterization

The bioactive glass composition of the binary system used in this Project, ($Di - CaMgSi_2O_6$) – *Tricalcium phosphate* ($TCP - 3CaOP_2O_5$) with the proportion of 70:30, is presented in Table 2.

***Table 2. Weight percentage composition of the Di70-TCP30 bioactive glass.***

| ***%wt.*** | $\boldsymbol{SiO_2}$ | $\boldsymbol{CaO}$ | $\boldsymbol{MgO}$ | $\boldsymbol{P_2O_5}$ |
|---|---|---|---|---|
| ***Di70-TCP30*** | 38.84 | 34.40 | 13.04 | 13.72 |

As mentioned in section §4.1 of the previous Chapter, this glass composition aim to overcome the main disadvantages related to other oxides combinations, especially the ones containing alkali. From this point of view the binary system of Di-TCP could be considered as a promising solution: it's been verified that Diopside based ceramics exhibit no general toxicity, help bone regeneration, as they contain elements which already compose bone tissue, and show great mechanical strength, even higher than hydroxypatite (8) (31) (49).

Raw materials for the glass powder production are reagents that contain the oxides presented in the table above: SiO2, CaCO3, MgO and NH6PO4.

Homogeneous mixtures of glass reagents to obtain 80 g of glass were produced by ball milling for 10 minutes. Afterwards, the powder has been transferred to an alumina crucible for calcination at 850ºC for 2 hours (2ºC/min rate) and then the material was melted in platinum crucible with a three-step heating process: first 10ºC/min rate from 20ºC to 1200ºC, then 5ºC/min rate until 1570ºC, followed by a 2 hours' dwell. The following quenching in cold water of the melted glass permitted to obtain glass frits, which were then dried in an oven at 100ºC for 24 hours.

The robocasting machine requires the creation of a homogenous paste able to be extruded through the nozzle. It's clear that the glass particle size and distribution play the principals roles. In order to avoid the clogging, to improve the packing of particles and to obtain a stable suspension, the glass went through different processes of particle size reduction. The frits were first milled in a planetary ball milling machine in dry conditions for 2 hours at a speed of 200 rpm (Retsch PM 400). The powder obtained was sieved (<40 µm) and its mean size was determined by a light scattering technique (Coulter LS230, Beckman Coulter; Fraunhofer optical model), being of about 4-5 µm.

These fine glass particles were in part stored and in part submitted to an attrition milling in order to further decrease the particle size, the powder was milled in an attrition milling device for about 16 hours at a speed of 500 rpm, in ethanol; the solution of powder and ethanol was dried out again at 100ºC for 24 hours and then sieved (<40 µm) to eliminate agglomerates. The powder obtained had a mean size of about 1 µm.

The amorphous nature of the glass frits was analysed by X-ray diffraction (XRD) analysis (Rigaku Geigerflex D/Max, Tokyo; Kapan; C Series, CuKα radiation; 2α angle range: 10º-80º; step: 0.02º/s).

The great advantage in the use of bioactive glass for scaffold production is their ability to strongly interact with the human body fluids and permit the formation of a hydroxyapatite layer on its surface: this will facilitate the subsequent bone tissue regeneration. The mechanism of this effect is not yet fully explained, even if different researches were done (50) (51) and showed that basically consists in 12 stages of reactions which occur in the material-tissue interface. Every step of the HA layer mechanism formation has a different speed; in a general way, it's possible to state that the rapidity of these stages is related to the

bioactivity of the material: since this property defines the response after the contact with living tissue, higher the bioactivity and faster will be the creation of the HA layer.

From this point of view, it's necessary to underline how the choice of the material with right surface properties and behaviour, in particular with the adequate biological response, is very important. One of the novelties in this Thesis is the implementation of an alkali-free bioactive glass; as stated in the previous Chapter, this choice is related to the numerous disadvantages associated with the presence of alkaline (mainly Na+ ions) in a biodegradable scaffold. From the phase point of view, it has been shown how this type of element, inside the glass, influences the sintering process (44): the low difference between the crystallization and glass transition temperature imply a greater crystallization over the densification mechanism of the bioglass and therefore, the alkali content in the glass lead to a higher presence of crystal structure. Since this phase affects the bioactivity and tends to decrease the rate of the HA layer formation as already mentioned, it is clear that the main point on the bioglass production is to obtain an almost fully amorphous structure.

After, Differential Thermal Analysis (DTA) and Thermogravimetric (TGA) were made on the glass in the equipment present in the Laboratories: Seteram Labsys DTA/TG-DSC, with a heating rate of 10ºC/min, from 25ºC to 1000ºC.

The aim of these analyses was to identify the nature of the reactions that could occur during the heating process and the relevant temperatures at which the principal transformations take place. The mass variation upon heating and the associated thermal effects were investigated.

## *1.1. CMC Solution Preparation*

As previous stated, carboxymethylcellulose is a compound made of polymeric chains and can be found with different molecular weight. The type used in this Project was the CMC 250 (Mw=250,000) in the powder state but many difficulties were encountered in the realization of a homogeneous mixing of CMC and water, due to its strong tendency to agglomerate (14). In order to facilitate and speed up the creation of the final paste, a *stock* solution was prepared containing the amounts required for preparing suspensions with 50% vol.% solids and containing added CMC amounts of 2 wt.% and 3 wt.%.

## 1.2. Suspension Preparation

The suspensions analysed were subjected to a process of deagglomeration in a planetary centrifugal mixer machine (THINKY, Japan) during subsequent steps of work, in order to obtain a homogeneous and smooth paste. For this reason, it was decided to prepare the suspension in the following manner:

(i) the amounts of CMC and water (if requested) are added in the container and mixed for 4 minutes at 1200 rpm
(ii) cycles of 4min at 700 rpm and of 4 min at 1200 rpm were used in 4 steps, while half of the powder of each (4–5 and 1 μm, in sequence) was added at every round
(iii) a final cycle of 2 min at 1200 rpm was made in order to obtain a more uniform suspension

In order to cool down and allow the rehydration of the paste, it was maintained in fridge temperatures (4-14°C) for 15 minutes and then prepared for the scaffold printing process.

## 1.3. Characterization

The main issue related to the creation of a suspension was to get a homogeneous paste-like system, able to be implemented in the robocasting machine. Many attempts were made in order to create an "ink" with a unique particle size, but results obtained were not satisfying enough, nor easily reproducible. For these reasons and in the interest of improving the packing between particles, a 50:50 wt.% mixture of two bioactive glass powders with mean sizes of ~1 μm and 4–5 μm was used.

After this selection, the study proceeded by preparing suspensions with increasing total amounts of solids and of CMC aiming at finding the most appropriate dispersion conditions for processing Di70-TCP30, namely maximizing the solids loading while keeping a suitable flow behaviour for the extrusion of the pastes through the fine nozzles. Table 4 summarises the different suspensions tested.

The effects of the different solid and additive combinations in the gelification behaviour of the suspensions were analysed through rheological measurement methods in oscillatory way (Kinexus, Malvern, United Kingdom) at room temperature, with cutting tension between 0.1

and 1000 Pa in order to determine the *linear viscoelastic region* (LVE), at an oscillatory frequency of 1Hz, with a plate/plate testing combination.

Viscosity tests were also made in order to verify the shear tinning behaviour of the created suspensions, by analysing them by varying the shear rate from 0 to $400s^{-1}$ at room temperature.

***Table 3. Illustration of the different combination of Vol. % of solids and wt. % of CMC studied.***

| Vol. % water | Vol. % solid | Wt. % CMC |
|---|---|---|
| 60 | 40 | 2 |
| 60 | 40 | 3 |
| 57 | 43 | 2 |
| 57 | 43 | 3 |
| 56 | 44 | 3 |
| 55 | 45 | 2 |
| 55 | 45 | 3 |
| 52 | 48 | 2 |
| 50 | 50 | 2 |

.

## 2. Scaffold production and characterization

The alkali-free bioactive glass scaffolds were produced by using a robotic deposition machine, the 3D Ink, LLC, which allows, by the use of the Robocad software, the creation of different structures, with desired porosity size. In this Project, three variants were printed: 300µm, 400µm and 500µm.

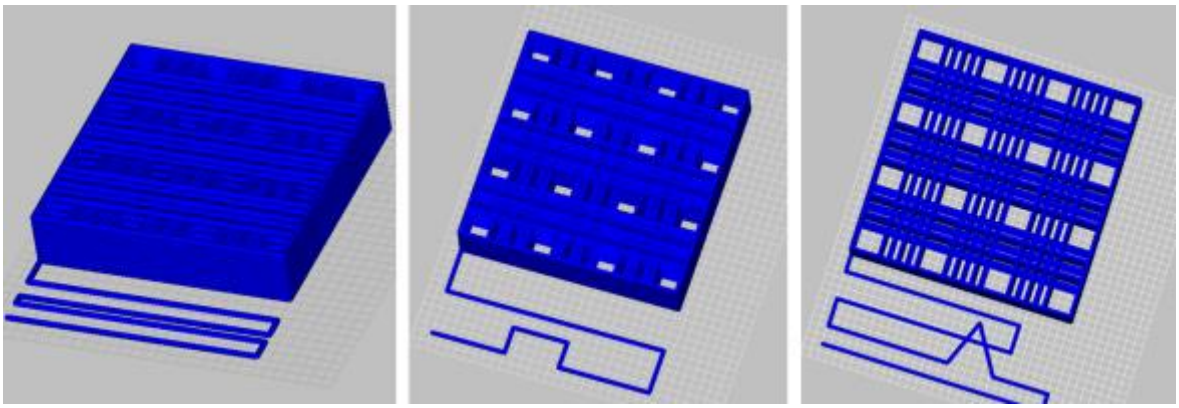

***Figure 5. CAD model of the scaffold printed with three different porosities: 300µm (a), 400µm (b), 500µm (c)***

For the realization of the scaffold structure were used the parameters showed in the following Table 4 and illustrated in the Figure 5.

***Table 4. Design parameters for the scaffold production.***

| **Design Parameter** | **µm** | | |
|---|---|---|---|
| **Porosity Size (a)** | 300 | 400 | 500 |
| **Filament Width (b)** | 410 | 410 | 410 |
| **Distance between filaments (c)** | 710 | 810 | 910 |

The suspension, previously produced, was inserted in a 5mL syringe and placed in the robocasting machine; in order to avoid a differential drying of the different layers, the paste was printed on a plate flood in an oil bath. After the deposition, the scaffolds were extracted and let to dry at room temperature for 48 hours.

Following, scaffolds were subject to a phase of sintering made of different temperature step and heating rate: first, with 5°Cmin$^{-1}$ until 200°C, then until 600°C at a heating rate of 0.4°Cmin$^{-1}$, and a final step at 2°Cmin$^{-1}$ until 800°C.

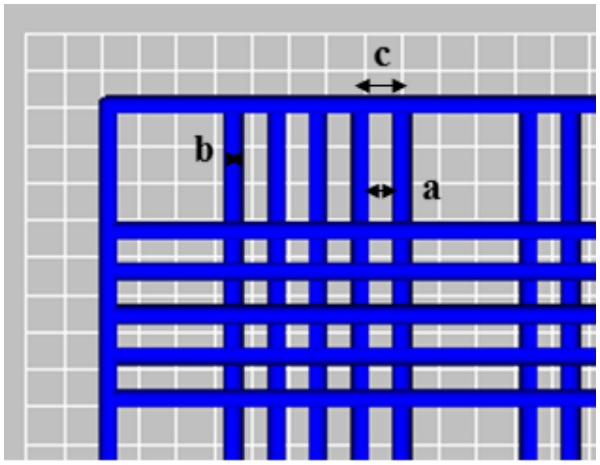


***Figure 6 . Illustration of the design parameters on the 3D scaffold***

Once the scaffolds went through sintering, they were characterized in terms of microstructure, pore size, porosity. The evaluation of mechanical strength under compression will be performed in a near future after the defence in order to complete gathering all the required data for writing and publishing a scientific article.

## *2.1. Microstructure*

The microstructure was observed with *Scanning Electron Microscope* (SEM) technology, by analysing the transversal section of the printed scaffolds, after they were subjected to the adequate sample preparation: they were fixed with double sided carbon glue in aluminium sample holder and covered with a carbon film obtained in a carbon evaporator machine (EMITECH K950).

## *2.2. Pore Size*

The pore size after sintering was checked through the SEM images, by using a digital elaborator program for images, the ImageJ software. The total shrink was calculated with the following equation:

$$S_{\%} = \frac{w_i - w_f}{w_f} \cdot 100 \qquad (2)$$

Where $w_i$ and $w_f$, correspond respectively to the initial (after deposition, settled in the robocasting machine) and final (after sintering) pore size.

## 2.3. Porosity

Subsequently, density tests were made in order to determine the porosity of the final obtained scaffolds, physical parameter directly related to the strength of the sample itself. Starting from the values of mass and volume of the sintered bodies, the apparent density was determined; since the theoretical density of the bioactive glass used is known from literature to be 2,92gcm$^{-3}$, it's possible to calculate the porosity percentage of the scaffolds with the following equation:

$$P(\%) = \left(1 - \frac{\rho_{apparent}}{\rho_{theoretical}}\right) \cdot 100 \quad (3)$$

For the calculation of the apparent density, mass and volume is requested. In order to do this, the sintered scaffolds were firstly cut in 9 cubes, same which will after undergo the mechanical tests. The value of the sample mass was obtained by using a laboratory analytic balance, while the volume was arithmetically established after the evaluation of the three dimensions (a, b, c) of the sample with a digital calliper. Both for the mass and for the volume determination, three measures were taken and then just the average value will be used in the numerical calculation.

***Table 5. Average values of the sample dimensions and weight.***

| | *a [mm]* | *b [mm]* | *c [mm]* | *V [mm$^3$]* | *m [gr]* |
|---|---|---|---|---|---|
| *300µm* | 2.7 | 2.7 | 3.2 | 22.5 | 0.0313 |
| *400µm* | 2.9 | 2.9 | 3.1 | 25.5 | 0.0324 |
| *500µm* | 3.3 | 3.2 | 3.1 | 32.7 | 0.0384 |

## *2.4. Mechanical Strength*

The samples, in form of cubes, were subject to compression tests in order to evaluate the Young's Modulus and the mechanical strength. To accomplish this, a general mechanical tester machine, SHIMADZU AG-IS, with speed of load application of 0.5mm.min$^{-1}$ and a load cell of 5kN, was implemented.

The value of the tension, is given by the ratio of the force applied per area unity (defined by the *a* and *b* parameter), given respectively from the machine acquired force data and the calculated transversal section subjected to the applied load. It's valid the following equation:

$$\sigma(MPa) = \frac{F}{A} \tag{4}$$

The material deformation can be expressed as the ratio between the height variation, before and after the compression test, and the initial height of the sample:

$$\varepsilon = \frac{\Delta h}{h_0} \tag{5}$$

Consequently, the Young's Modulus can be calculated with the following equation:

$$E = \frac{\sigma}{\varepsilon} \tag{6}$$

It's necessary to underline that, due to the time spent on the analysis of the rheological properties of the different combinations of the suspensions, it was not possible to determine the mechanical strength of the produced scaffolds.

# CHAPTER 4

# Results and Discussion

In this Chapter data obtained from the described tests will be presented, including also powder particles size distribution. The behaviour and character of the suspension analysed will be illustrate with the viscosity and oscillation tests. The decisions made in the Experimental approach will be explained as well as the discussion of the obtained values.

## 1. Glass Characterization

### *1.1. Crystallographic Analysis*

The spectra obtained from the X-rays done on the bioactive glass frits, illustrated in Figure 7, shows the absence of crystal phase, confirm, in this way, the amorphous structure of the glass quenched in water. In order to obtain a biocompatible scaffold it's necessary that the amorphous phase of the

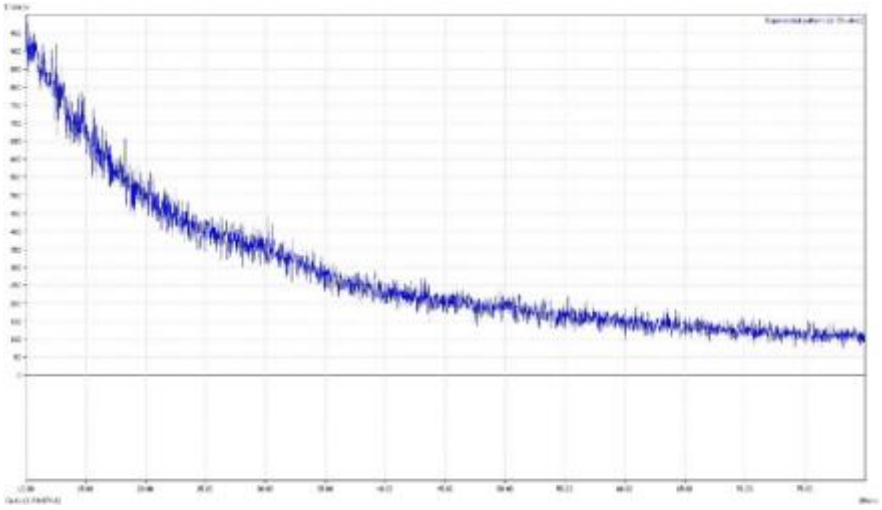

***Figure 7. XRD of the Di70-TCP30 bioactive glass, with amorphous structure.***

material is mantained after the sintering process. For this reason an XRD analysis was made over the sintered scaffold and shown in Figure 8, the amorphous structure is mantained.

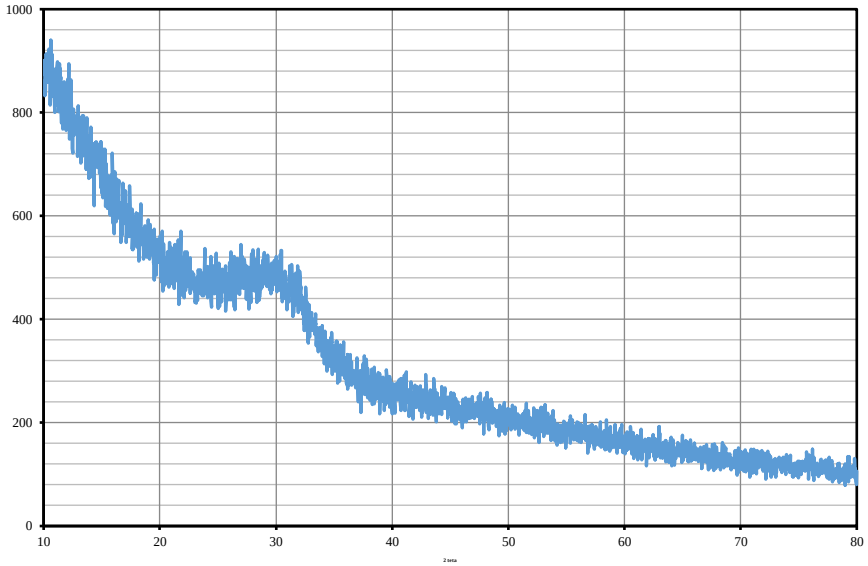


***Figure 8. XRD of the Di70-TCP30 bioactive glass after sintering, with amorphous structure.***

## 1.2. Size Reduction and Granulometric Analysis

In order to prepare a suspension able to be implemented in the robocasting machine, it's necessary to reduce the frits size to a micrometer scale. Therefore, the glass frits went through subsequent comminution stages until obtaining the desired small particle sizes.

The most challenging issue encountered in this Project was the realization of a stable and with adequate rheological characteristics paste. In this sense, it's possible to generally define two main requirements to produce a correct suspension:

(i) The system inserted in the syringe and then extruded through the nozzle must present a shear thinning behaviour in order to not clog the pin and be easily deposit by the robocasting machine

(ii) Since the main final purpose of this work is to realize a scaffold for bone tissue regeneration, the printed body must present a minimum strength in order to act as an adequate replacement of the tissue functions, until their complete restoration.

In term of paste production these demands strongly depend on the particle size and distribution. In fact, as well investigated (15) (16), these properties totally affect the rheological properties. In particular, it's possible to assert that bigger the particle size, easier

will be the realization of the paste but higher will be also the risk to obtain a system with a shear thickening behaviour and lower will be the maximum solid loading. On the other hand, finer the particle size and more difficult will be the work required to obtain a homogeneous dispersion of the material in suspension, since, cause of their high surface energy, they tend to strongly interact and attach to each other, already discussed in Chapter 2. From this perspective, using a combination of two different average particle sizes, allows a better packing of the system, and therefore, enables increasing the solid loading in order to get a better mechanical behaviour of the final printed scaffold (17) (18).

The milling process is fundamental, as stated previously, in order to have control on the particle size and distribution, and consequently regulate the rheological behaviour of the paste. Therefore, two powder frits, one with a mean particle size of 1 µm, and the other with a mean particle size of 4-5 µm were mixed in a 1:1 weight ratio to prepare the suspensions.

In Figure 8 is showed the particle size distribution obtained after submitting the glass frits for 1 hour and 2 hours at 200rpm in the planetary milling machine, in order to investigate the effect of dry milling time on particle size reduction.

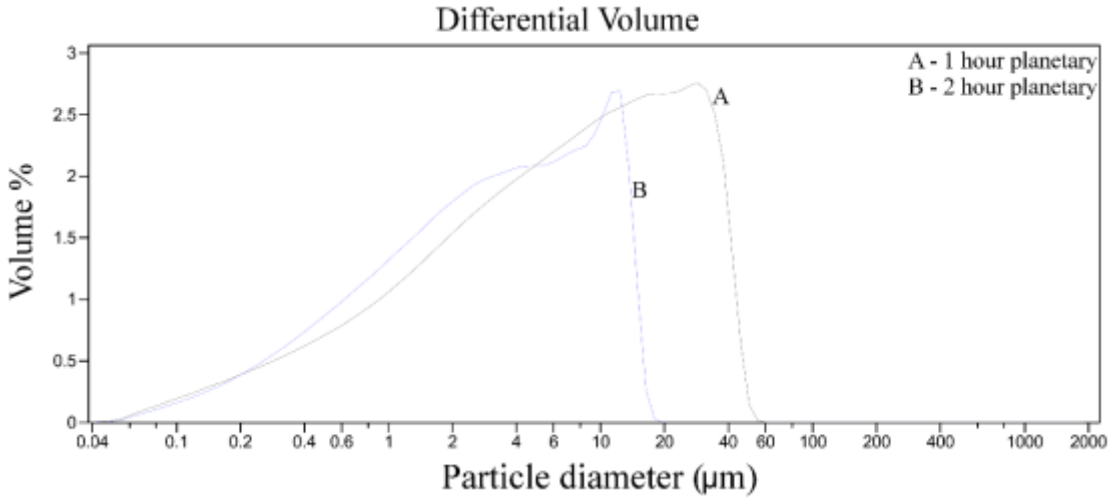


***Figure 9. Particle size distribution after different time of the bioactive glass in the planetary milling machine.***

This powder was then collected and milled again in the attrition milling machine. Figure 9 shows the evolution of the particle size distribution after different stages of time, until the mean size of about 1µm.

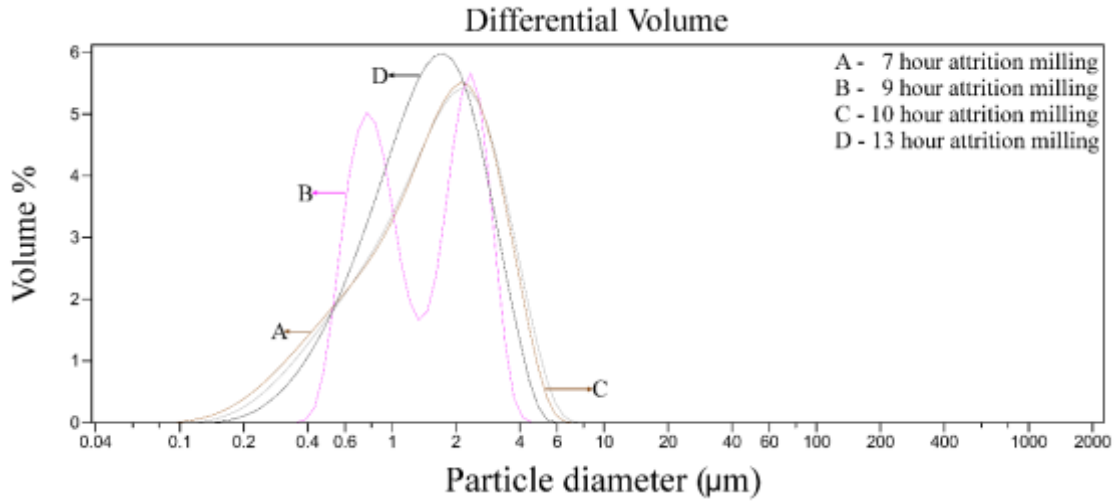


***Figure 10. Particle size distribution after different time of the bioactive glass in the attrition milling machine.***

## 2. Paste Characterization

The mechanism of surface interaction between different particles has been described in the §2 of the previous Chapter. It became clear that one of the main issue encountered in the experimental part of this Project was the creation of a paste with specific rheological behaviour, able to flow through the nozzle of the robocasting machine and to retain the shape designed in the CAD model, after deposition. On the other hand, after optimizing the particle size distribution, in order to gain a more packing system, the next step was aimed at increasing as much as possible the solid loading: higher this value and greater will be the mechanical response of the final scaffold. From this perspective, it was necessary to analyse the effect of different bioactive glass solid loadings on its rheological properties.

It is worthy underlining that the suspensions are composed of two part, the solid, composed by the glass powder and the CMC (which amount will be calculated as a weight fraction of the glass part), and the liquid, composed by distillated water. As well described in previous chapters, the CMC is the unique additive chose for this Project, as it can act both as dispersant and binder, depending on the amount added. From this point of view, starting from previous researches and studies related to the printing of bioactive glasses with CMC (7) (19), it was decided to firstly investigate the rheological properties of the paste with a fixed amount of CMC (2%), while varying the solid loading.

As mentioned, a paste is able to be implemented in the robocasting technique if it shows a shear thinning behaviour and, in order to obtain a final scaffold with adequate mechanical properties, the suspension must also present a suitable value of Elastic Modulus (G'). To verify the viscosity and visco-elastic behaviour, the paste was subjected to two different tests, respectively in viscometry and oscillatory mode of the rheometer.

In Figure 10, the results of the viscosity analysis are reported.

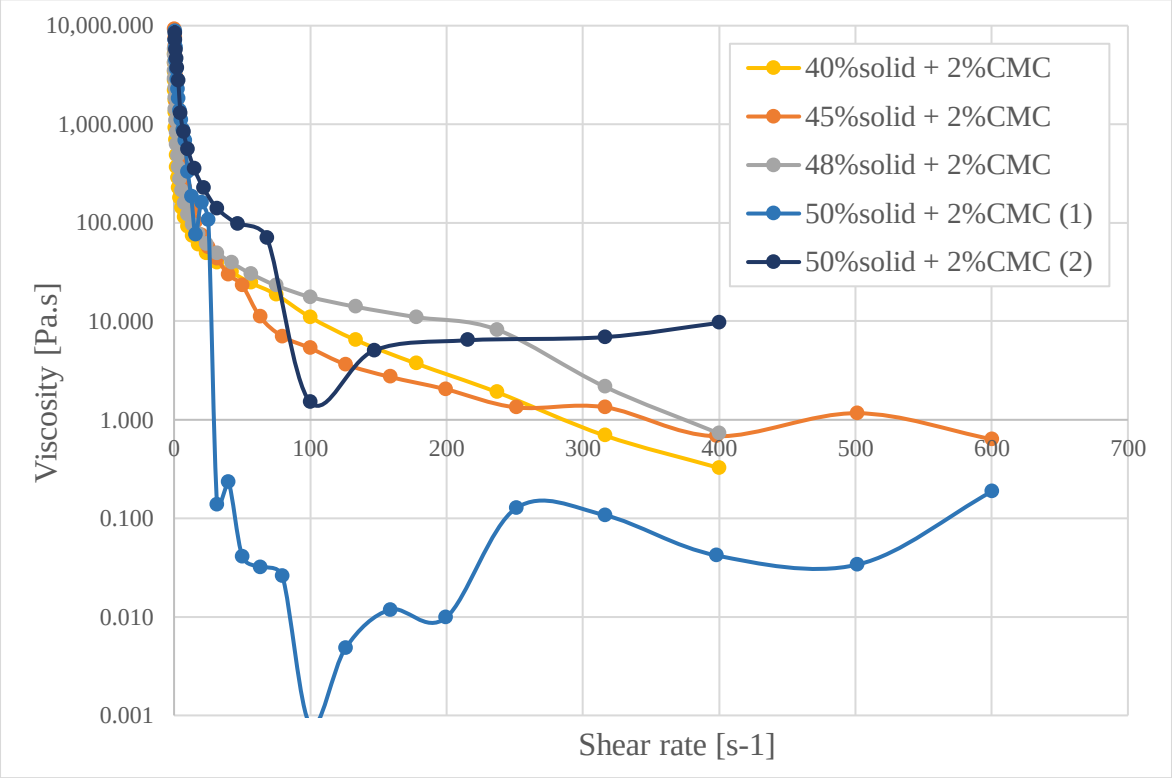


***Figure 11. Viscosity profile of suspension with increasing amount of solid loading and fixed quantity of CMC.***

It can be seen that all the tested suspension exhibit shear thinning behaviour: in fact, there's the tendency, in all the reported curves, to a decrease in the viscosity when they are driven to flow at high rates. As expected, with increasing solid loading, the viscosity profile tends to shift upper; the increased volume occupied by the glass particles lead to a less viscous and more elastic system.

Thanks, moreover, to the great packing of the paste, due to the dual particle size used for its production, it was possible to analyse a wide variation of the solid loading, starting from

40%vol until reaching the 50%vol. It must be underlined however the irregular and anomalous behaviour of the 50%vol solid suspension: the viscosity tends to decrease with increasing shear rate but exhibit, at $100s^{-1}$, a drop and variation of the past attitude, since the viscosity move to higher values. This strange behaviour it's possibly related to the high solid loading of this suspension and a trend for shear induced agglomeration. The resulting suspension becomes difficult to flow homogeneously under the applied shear stress and the observed drops are likely due to slippery effects of the measuring sensor that momentary loses adherence and contact with the suspension. When the contact between the measuring sensor and the testing suspension in a momentary re-established gives rise to the observed irregular increases in the viscosity. The anomalous flow behaviour of the system with 50 vol.% solids might also be due to some lack of initial homogenisation. Therefore, more stages of powder addition and mixing into the planetary machine have been used thereafter in the preparation of the suspensions. From this point of view is clear how the dispersal of the particles more and more difficult as the solid volume fraction of the paste increase.

In order to determine the overall nature of the suspensions and to investigate how the solid loading affects the mechanical properties, oscillatory tests were carried out and the results are shown in the Figure 11.

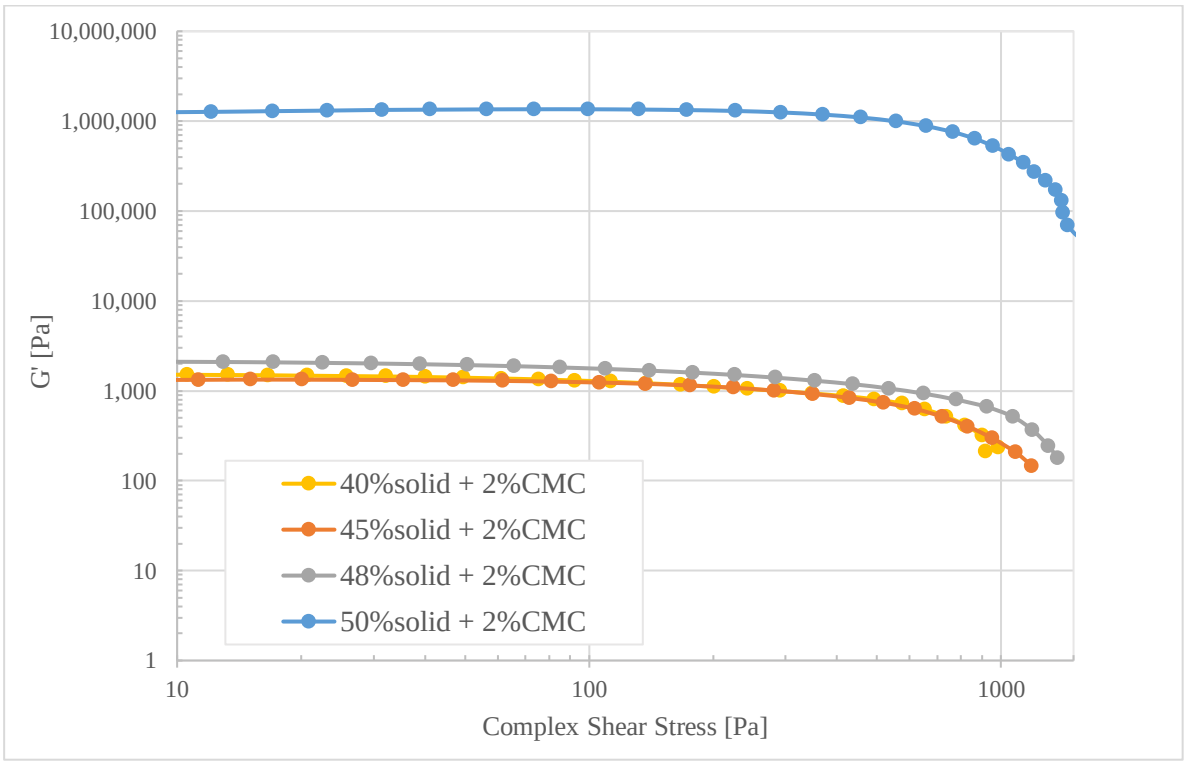


***Figure 12. Visco-elastic behaviour of suspension with increasing amount of solid loading and fixed quantity of CMC, analysed in the oscillatory mode.***

When a material is used in the robocasting machine, it's subjected to deformation during the extrusion process that partially destroy the system network, so it must flow under the applied pressure, but it must recover its structure and shape once deposited. The capacity of a paste to present this kind of behaviour is determined by the LVE region in the Elastic Modulus test. In fact, this can be approximated as the "working zone" of the material: it is represented by the shear stress range in which the value of elastic modulus is stable and consequently determines the condition region in which it's possible to assess the internal structure and judge about the stiffness of the paste and the shape retention capacity of the extruded filaments. The wideness of the LVE range determines if the material is able to withstand the robocasting applied pressure and also able to retain its shape after extrusion.

As the reported curves show, all the suspension combinations present a large work zone which is then suitable for robocasting: final inks stay stable along all the shear stress range tested, suggesting that the deposited filaments will be mechanically stable and capable of fully supporting their own weight during the assembly. The graph shows, however, a strange and non-expected evolution of G' with increasing solid loadings. As a matter of fact, the variations in elastic modulus when passing from 40 vol.% to 45 vol.% and 48 vol.% are relatively small. A further increase in solid loadings to 50 vol.% led to a significant jump in G', which would enhance the mechanical stability of the scaffolds. However, once this paste was loaded into the syringe it was not capable to be extruded due to its high stiffness.

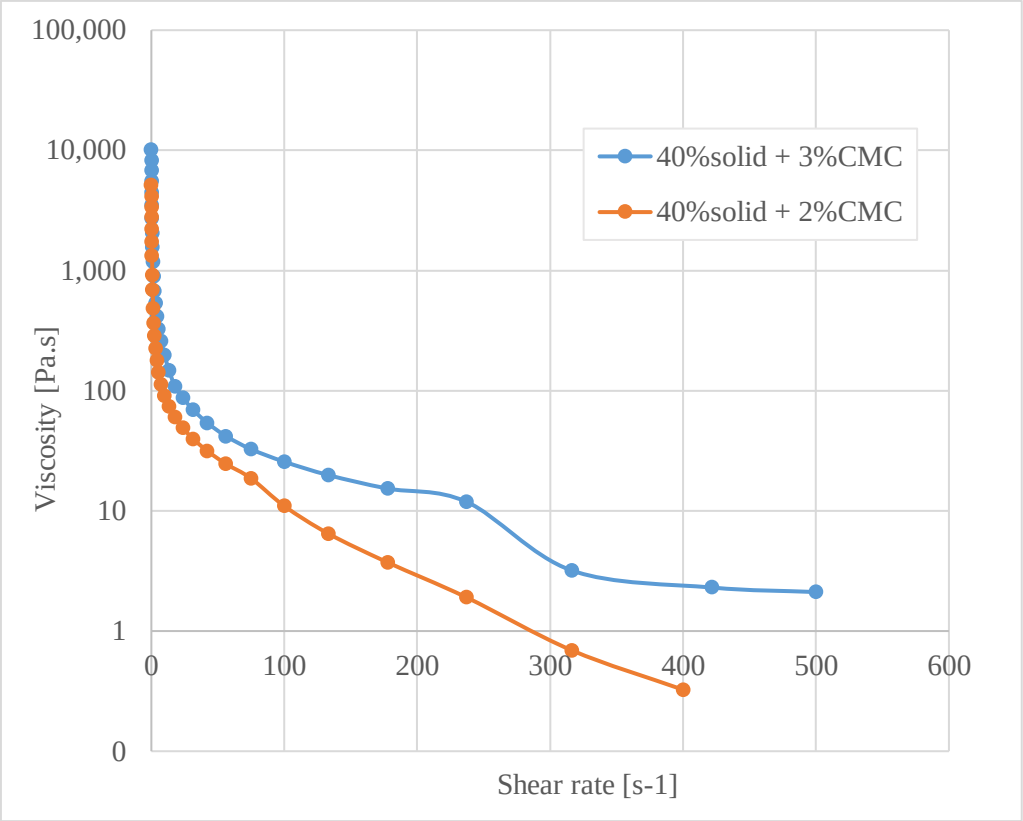


***Figure 13. Effect of the increased amount of CMC with fixed solids loading.***

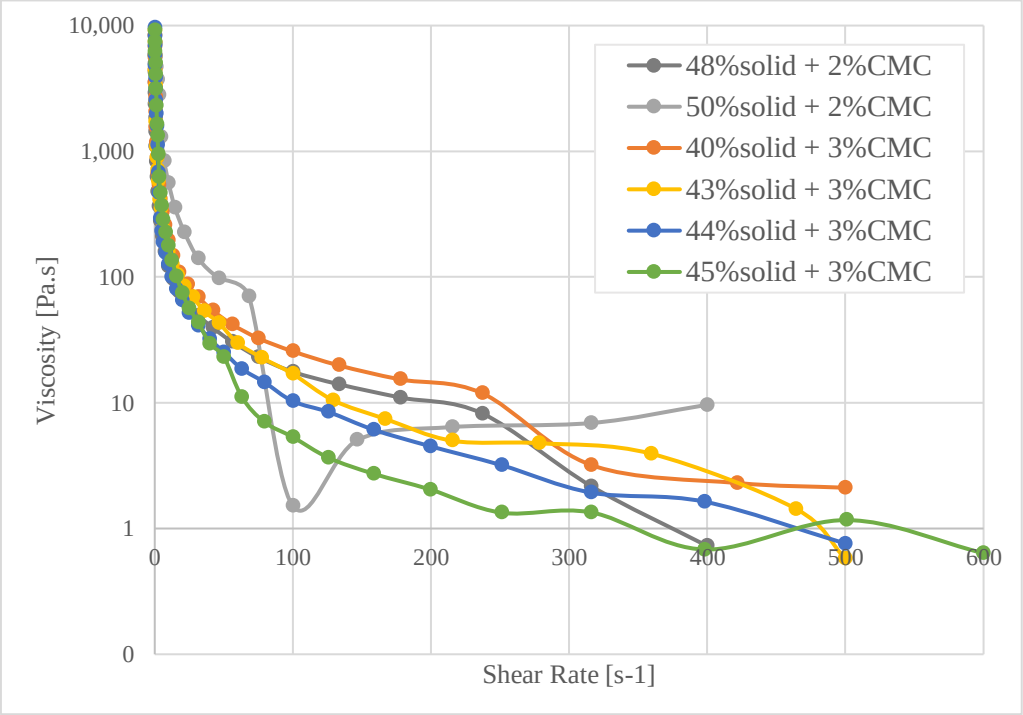


***Figure 14. Viscosity profile of suspension with increasing amount of solid loading and variable quantity of CMC***

With the purpose to both reach the maximum possible solid loading and to obtain an extrudable paste, it was decided to analyse what was the effect of the variation of CMC amount and the solids volume fractions. Figure 12 and Figure 13 display the apparent viscosity curves of suspensions with solids loading within the range of 40-45 vol.% and containing 3 wt.% CMC and compares them with those of suspensions containing 2 wt.% CMC and 48-50 vol.% solids. It is possible to observe that the overall shear thinning behaviour was conserved in all systems. But again, the same slippery effect observed in Figure 10 have apparently occurred for the most concentrated suspension. It must be underlined also that the flow curves became smoother when the added amount of CMC was increased to 3 wt.%. these results suggest that particles start colliding more often whit each other under flow conditions when the solid loading is increased due to their closer proximity, gradually hindering the flow. Increasing the amount of CMC in the dispersion liquid enhances its intrinsic viscosity, limiting the total achievable concentration of solids, while tending to hinder particle segregation. Therefore, optimizing the flow behaviour is a trade of suitably combining the right amounts of solids and processing additive for a given particle size distribution. On the other side, the use of a plate/plate system in the rheometer influence the profiles and tend to be less trustable than a cone/plate combination in the measurement of the viscosity.

As reported in Figure 14, all the tested combination of solid loading with 3%CMC as additive show an elastic response that fill the gap between the 48%vol and 50%vol with 2%CMC:

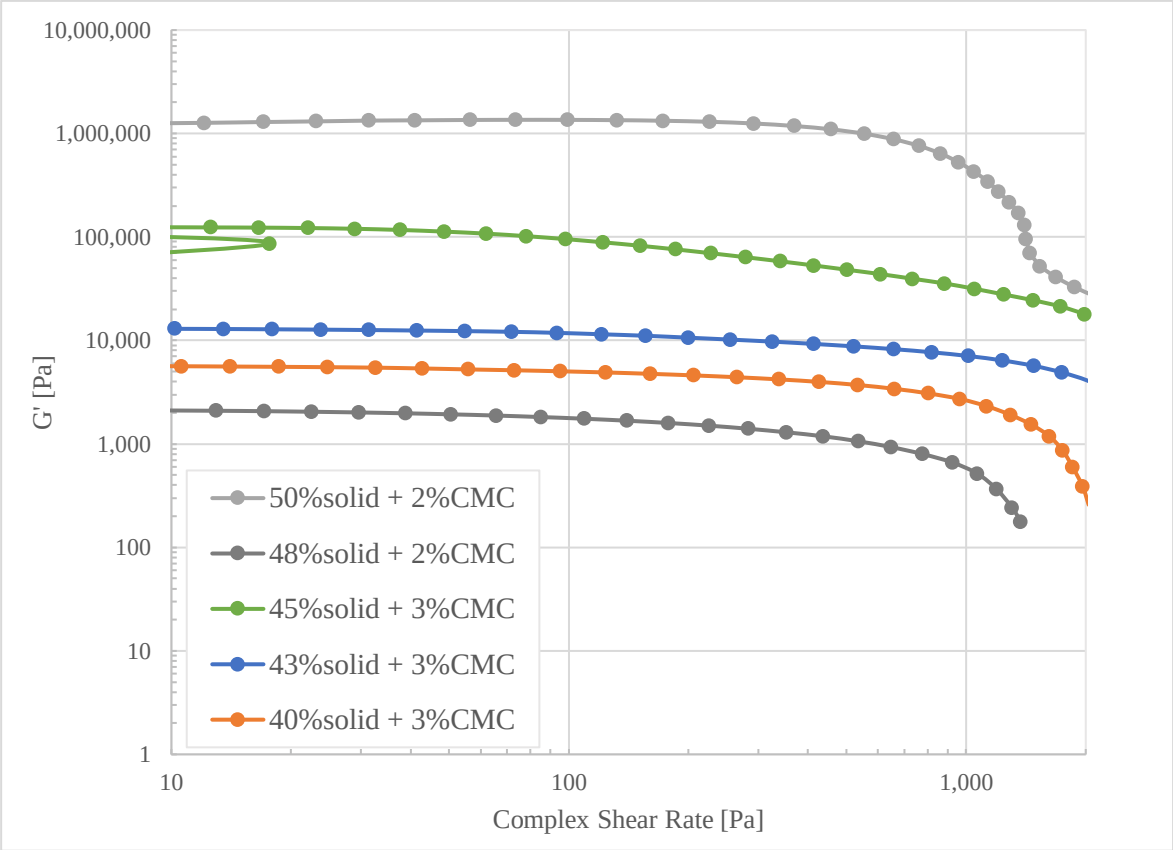


***Figure 15. Visco-elastic behaviour of suspension with increasing amount of solid loading and variable quantity of CMC, analysed in the oscillatory mode.***

These curves reveal that it is possible to reach high G' values even with the lowest solid loading (40%) provided that the amount of CMC is increased to 3 wt.%. this confirms that playing with solid loading and the added amount of processing additive enables formulating suitable pastes for additive manufacturing by robocasting. The pastes contain 3 wt.%CMC exhibit intermediate G' values among the extreme cases of pastes with added 2 wt.%CMC. From this point of view, the graph (Figure 14) shows as promising solutions the suspensions with 43 vol.%, 44 vol.% and 45 vol.% solids. However, when attempting to print using the systems with 44 vol.% and 45 vol.% solids, handling of the pastes upon filling the syringes was difficult and extrusion of these pastes was not possible. For these reasons, it was decided to work, print and analyse just one combination: the 43 vol.% solid loading with 3 wt.% CMC.

# 3. Scaffold Characterization

## *3.1. Morphologic Analysis*

The shape stability of the extruded filaments can be inferred from the SEM images of scaffolds after deposition (*green sample*) are shown in Figure 15.

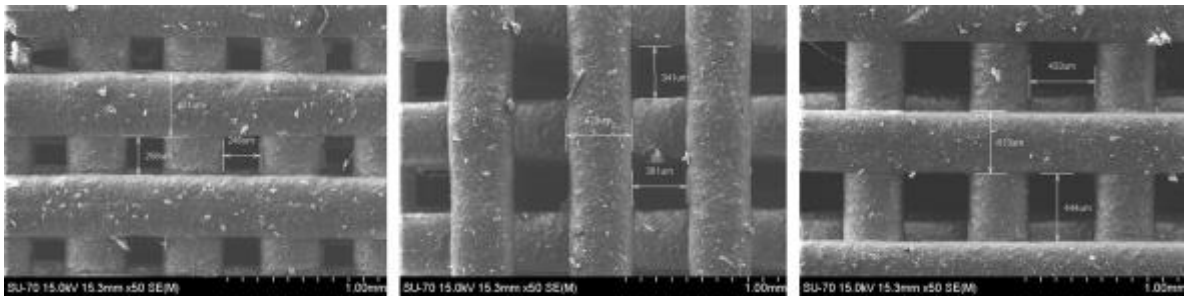

***Figure 16. Magnification of printed scaffold before sintering with different porosity; (a) 300µm, (b) 400µm, (c) 500µm.***

It can be seen the filament size is approximately the same as that of the extrusion nozzle dimension (410µm). the measured small differences can be attributed to shrinkage upon drying and eventual small deformation of the filaments upon extrusion. The pore size tends to be reduced in respect to the one imposed in the CAD program. This is expected as the overall dimensions of scaffolds are reduced upon drying. However, all SEM micrographs reveal structures with well-defined and interconnected pores, an important feature to allow a good vascularization. The deposited filaments were mechanically stable and capable of fully supporting their own weight during the assembly, as deduced from the absence of significant shape deformation caused by overlapping the other layers, as shown in Figure 15, with the side section of the scaffolds.

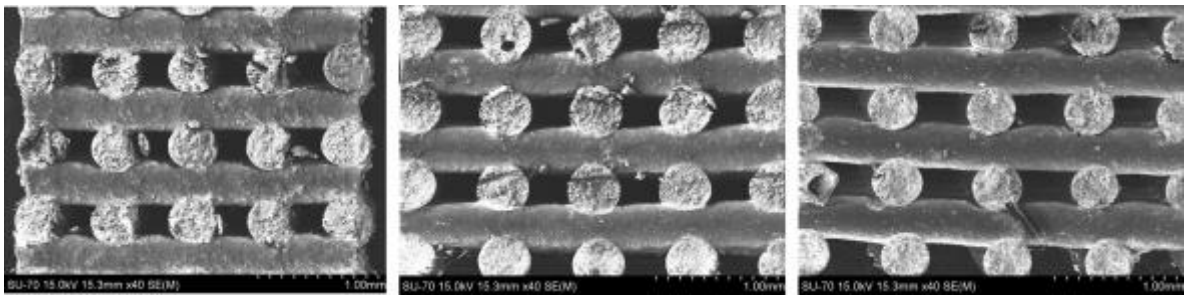

***Figure 17. Side section of printed scaffolds before sintering with different porosity; (a) 300µm, (b) 400µm, (c) 500µm.***

The same measurements were made for the scaffolds after sintering; results are reported in Figure 17 and Figure 18.

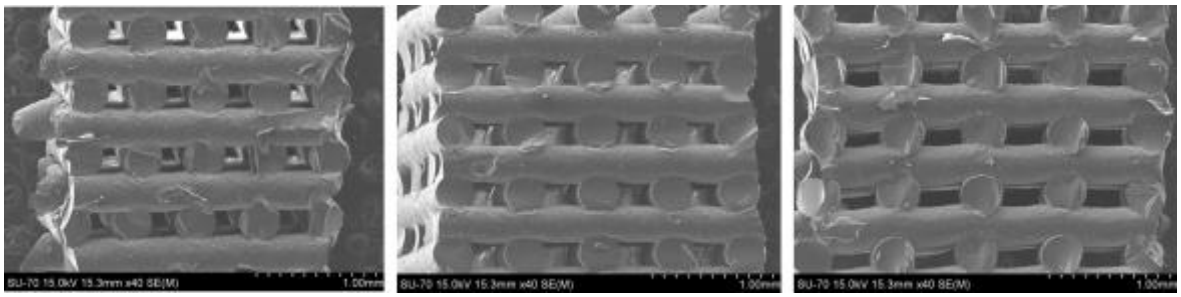

***Figure 18. Side section of printed scaffolds after sintering with different porosity; (a) 300µm, (b) 400µm, (c) 500µm.***

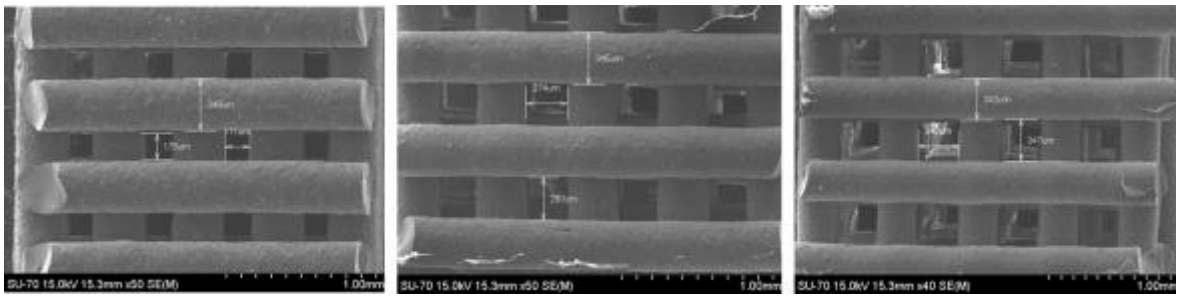

***Figure 19. Magnification of printed scaffold after sintering with different porosity after sintering; (a) 300µm, (b) 400µm, (c) 500µm.***

The SEM micrographs also provide evidences about the good adhesion between adjacent layers: features which are essential for obtaining 3D sintered structures with strong mechanical properties. The filaments section is generally dense, but it's possible to see also some isolated pore, due to a not precise removal of all the air bubbles presented inside the syringe during the paste loading.

## *3.2. Pore Size*

Thanks to the SEM pictures obtained, it was possible to calculate the pore size of the scaffold before and after sintering and consequently determine its shrinkage during the heating process. Table 6 shows the values. As expected, due to the relative low amount of solid loading into the paste, after the sintering process the scaffold tend to be subjected to a shrinkage effect.

***Table 6. Pore sizes calculated from the SEM images and relative shrinkage in case of different porosity***

| Theoretical size | Before | After | Shrinkage |
|---|---|---|---|
| **300** | 252±6 | 173±2 | 45.6% |
| **400** | 351±10 | 282±8 | 24.5% |
| **500** | 439±6 | 345±3 | 27.5% |

## *3.3. Porosity*

The porosity fractions of the scaffolds were calculated as it has been described in Chapter 3. A scaffold, intended to be used as a temporary substitute of the bone tissue engineering and regeneration must present an adequate porosity fraction: not too high to compromise the mechanical response, and not too low to prevent ions and cells diffusion and their optimal growth. The obtained values are presented in Table 7.

***Table 7. Pore size and porosity values calculated.***

| Pore size | Porosity |
|---|---|
| 300µm | 52.3% |
| 400µm | 56.5% |
| 500µm | 59.9% |

As expected the porosity tend to increase with the increasing of the space between rods but the values of the three-different scaffold are very similar to each other. However, due to the same reasons mentioned above for pore size and total shrinkage, the estimated values are affected by the same deformation events and the real porosity needs to be better evaluated using geometrical approaches and or on immersion measurements using the Archimedes principle.

## *3.4. Mechanical Strength*

The analysis of the mechanical properties of the sintered scaffolds is necessary in order to estimate its capacity to be used as a bone substitute. From this point of view, they must

possess a minimum compression strength enough adequate to sustain the loads that will have to support and a modulus of elasticity close to the native tissue, so that the distribution of loads is identical.

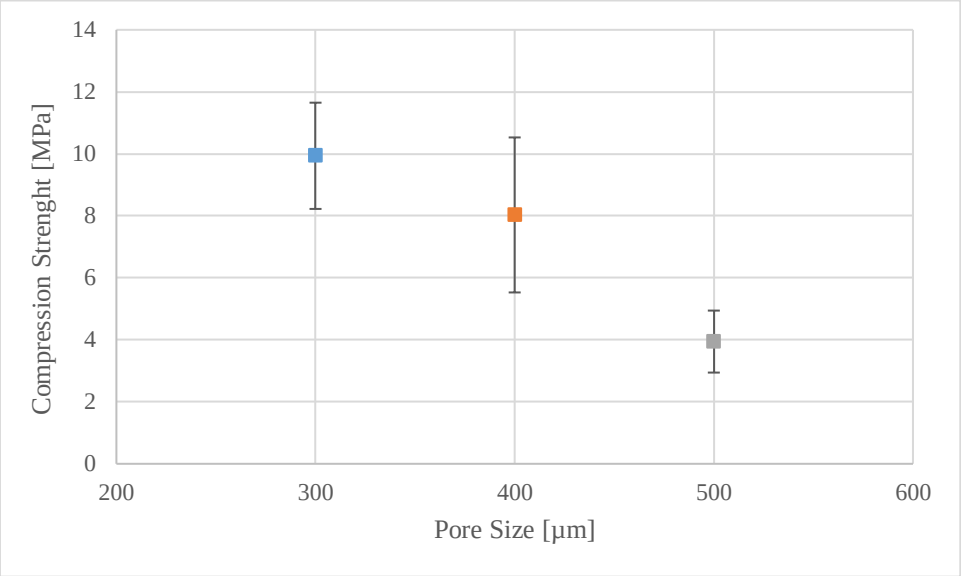


***Figure 20. Tensions values of the samples with different pore size.***

***Table 8. Tension values of the samples, refered to the different pore sizes.***

| Pore size [µm] | Compressive Streght [MPa] |
|---|---|
| 300 | 9.94 ± 1.71 |
| 400 | 8.03 ± 2.51 |
| 500 | 3.90 ± 0.42 |

As reported in Figure 19 and Table 8, the values of tension calculated have the expected trend: with the increasing of the pore size, and consequently the porosity (see Table 7), the tension tends to decrease.

Since the compressive strength of the spongy part of the bone structure varies between 2-12 MPa (20), it's possible to observe that all the tested scaffolds present strength values included in the range reported above and they could therefore be used as substitutes.

# Conclusions

The aim of this Master Thesis was the realization of 3D porous scaffolds made of alkali-free bioactive glass with the robocasting technique, in order the fabricate devices suitable for bone tissue regeneration. The study was then divided in different steps:

(i) Glass preparation through melt quenching technique and subsequent size reduction to state of micrometric powder. As proved and discussed, the particle size distribution represents a critical parameter in the creation of a dispersed suspension with controlled rheological behaviour. For this reason, a double sized glass powder was fabricated

(ii) Preparation of concentrated glass based suspensions and relative characterization. Starting from the requirements requested from the robocasting technique for the character and behaviour of the paste, many attempts were made in terms of glass and additive combinations, in order to obtain a satisfactory suspension

(iii) Fabrication of bioactive glass scaffolds with different porosity size with the robocasting additive manufacturing technique, with subsequent characterization

It became clear along this work that promising results could be obtained many by playing with the particle size distribution that controls the particle packing ability along the fabrication process. A 1:1 glass mixture of glass powders having mean particle diameters of 1 μm and 4–5 μm enabled preparing suitable suspensions by playing with the contents of CMC and solid loading. From the Viscosity and Elastic Modulus measurements it could be concluded that for a fixed overall particle size distribution, the other most determining experimental factors are the solids loading and the added amount of CMC. An added amount of 2 wt.% of CMC enables higher solid loading to be achieved, but the flow behaviour at the maximum solids loading revealed to be inadequate for the extrusion process, due to the high stiffness of the paste, shear induced aggregation and consequent slippage effects. On the other hand, decreasing solids loading in the presence of 2 wt.% of CMC caused accentuated decreases in the elastic modulus. In contrast, increasing the amount of CMC to 3 wt.% enables more gradual and controlled changes in the viscoelastic properties of the pastes while imposed lower limits for the maximum solid loading.

Robocasting technique revealed a good additive manufacturing technique permitting to exert a high control over the scaffold structure and internal porosity. The realized scaffolds present good characteristics. The shape of the extruded rods was reasonably preserved, and of the overall porous structure was maintained stable and uniform.

## *Future Work*

In order to define better the interaction forces generated between CMC and glass particles, a deeper analysis on the effective steric effect of the additive could help in the control of the rheological properties of the suspensions.

Other aspects that need to be better equated are related to the description of the structure of the scaffolds through more realistic measurements of porosity and shrinkage.

Although this selected bioactive glass composition has already demonstrated to exhibit excellent in vitro properties, it has never been tested with a scaffold structure. Therefore, it would also be interesting to investigate in vitro the effects of pore size on the differentiation and proliferation processes of hMSC. Similarly, in vivo studies would be worthy to be performed to test the suitability of the scaffolds for the intended applications.

# Bibliography


1. **Coleman, A.L. Boskey and R.** Aging and Bone. *Journal of Dental Research.* 2010, Vol. 12, 89.

2. *Osteoporosis and ischemic cardiovascular disease.* **Michel Laroche, Virginie Pécourneau, Hubert Blain, Véronique Breuil, Roland Chapurlat, Bernard Cortet, Bruno Sutter, Yannick Degboe.** 84, 2017.

3. **Rozalia Dimitriou, Elena Jones, Dennis McGonagle and Peter V Giannoudis.** Bone regeneration: current concepts and future directions. *BioMed Central.* 2011, Vol. 9, 66.

4. **Ami R. Amini, Cato T. Laurencin and Syam P. Nukavarapu.** Bone Tissue Engineering: Recent Advances and Challenges. *Critical Reviews™ in Biomedical Engineering.* 2012, Vol. 5, 40.

5. **Gurbinder Kaur, O.P. Pandey, K. Singh, Dan Homa, Brian Scott, Gary Pickrell.** A review of bioactive glasses: Their structure, properties, fabrication and apatite formation. *Journal of Biomedicl Materials Research.* 2013.

6. *The story of Bioglass.* **Hench, Larry L.** 11, 2006, Journal of Materials Science: Materials in Medicine, Vol. 17, pp. 967-978.

7. *A simple recipe for direct writing complex 45S5 Bioglasss 3D scaffolds.* **S. Eqtesadi, A. Motealleh, P. Miranda, A. Lemos, A. Rebelo, J. M.F. Ferreira.** 2013, Materials Letters, Vol. 93, pp. 68-71.

8. **Saurabh Kapoor, Ângela Semitela, Ashutosh Goel, Ye Xiang, Jincheng Du, Ana H. Lourenço, Daniela M. Sousa, Pedro L. Granja, José M.F. Ferreira.** Understanding the composition–structure–bioactivity relationships in diopside (CaO·MgO·2SiO2)–tricalcium phosphate (3CaO·P2O5) glass system. *Acta Biomaterials.* 2015, 15.

9. **College, OpenStax.** *Anatomy and Physiology.* 2013.

10. **Andrew, Warren.** *ENCYCLOPÆDIA BRITANNICA.* [Online] 27 Febbraio 2017. https://www.britannica.com/science/human-skeletal-system.

11. **Association, Aquatic Exercise.** *Aquatic Fitness Professional Manual-6th Edition* . 2010. 9780736067676.

12. **Goel A, Kapoor S, Rajagopal RR, Pascual MJ, Kim HW, Ferreira JM.** Alkali-free bioactive glasses for bone tissue engineering: a preliminary investigation. *Acta Biomaterials.* 2012, 8.

13. **Jan Mewis, Norman J. Wagner.** *Colloidal Suspension Rheology.* Cambridge : Cambridge University Press, 2012. ISBN 978-0-521-51599-3.

14. **Karolina Boruvkova, Jakub Wiener.** WATER ABSORPTION IN CARBOXYMETHYL CELLULOSE. *AUTEX Research Journal.* 2011, Vol. 11, 4.

15. **S.M. Olhero, J.M.F. Ferreira.** Influence of particle size distribution on rheology and particle packing of silica based suspensions. *Powder Technology.* 2004, 139.

16. **Ukeje, Paul F. Luckham and Michael A.** Effect of Particle Size Distribution on the Rheology. *Journal of Colloid and Interface Science.* 1999, 220.

17. **A.F. Lemos, JoséD. Santos, José M.F. Ferreira.** Influence of Characteristics of the Starting Hydroxyapatite Powders and of Deagglomeration Procedure, on Rheological Behaviour of HA Suspensions. *Materials Science Forum.* 2004, Vol. 455-456.

18. **J.Franco, P.Hunger, M.E.Launey. AuA.P.Tomsia, E.Saiz.** Direct write assembly of calcium phosphate scaffolds using a water-based hydrogel. *Acta Biomaterialia.* 2010, Vol. 6, 1.

19. **Siamak Eqtesadi, Azadeh Motealleh, Pedro Miranda, Antonia Pajares, Alexandra Lemos, José MF Ferreira.** Robocasting of 45S5 bioactive glass scaffolds for bone tissue engineering. *Journal of the European Ceramic Society.* 2017, 37.

20. *Biology of Bone Tissue: Structure, Function, and Factors That Influence Bone Cells.* **Rinaldo Florencio-Silva, Gisela Rodrigues da Silva Sasso, Estela Sasso-Cerri, Manuel Jesus Simões and Paulo Sérgio Cerri.** s.l. : BioMed Research International, 2015. PMC4515490.

21. **Zartner P, Cesnjevar R, Singer H, Weyand M.** First successful implantation of a biodegradable metal stent into the left pulmonary artery of a preterm baby. *Catheter Cardiovasc Interv.* 2005, Vol. 4, 66.

22. *Evaluation of mechanical strengths of three types of mini-implants in artificial bones.* **Yu-Chuan Tseng, Ju-Hui Wu, Chun-Chan Ting, Hong-Sen Chen, Chun-Ming Chen.** 33, 2017, Medical Sciences, p. 96-101.

23. **Vogel M, Voigt C, Gross UM, Müller-Mai CM.** In vivo comparison of bioactive glass particles in rabbits. *Biomaterials.* 2001, 22.

24. **Tsutsumi, Toru NonamiSadami.** Study of diopside ceramics for biomaterials. *Journal of Materials Science: Materials in Medicine.* 1999, Vol. 10, 8.

25. **Tony M. Keaveny, Wilson C Hayes.** Mechanical properties of cortical and trabecular bone. *Bone, Volume 7: Bone Growth-B.* s.l. : CRC Press, 1993.

26. **T. Kokubo, H. Kushitani, S. Sakka, T. Kitsugi, and T. Yamamuro.** ”Solutions able to reproduce in vivo surface-structure changes in bioactive glass-ceramic A-W. *Journal of Biomedical Material Research.* 1990, 24.

27. **T, Nakashima.** Regulation of bone homeostasis by bone cells. *Clinical Calcium.* 2013, Vol. 2, 23.

28. **SF., Gilbert.** *Developmental Biology. 6th edition.* Sunderland : Sinauer Associates, 2000.

29. **Services, U.S. Department of Health and Human.** FDA. *FDA US Food Drug Administration.* [Online] 24 Giugno 2015. https://www.fda.gov/MedicalDevices/ProductsandMedicalProcedures/ImplantsandProsthetics/default.htm.

30. *In Vitro Dissolution of Melt-Derived 45S5 and Sol-Gel derived 58S Bioactive Glasses.* **Sepulveda, P.** 61, 2002, J Biomed Mater Res, Vol. 2, p. 301-311.

31. *Potential of biomimetic surfaces to promote in vitro osteoblast-like.* **S. Hattar, A. Asselin, D. Greenspan, M. Oboeuf, A. Berdal, J.-M. Sautier.** 26, 2005, Biomaterials, p. 839-848.

32. *Robocasting of 45S5 bioactive glass scaffolds for bone tissue engineering.* **S. Eqtesadi, A. Motealleh, P. Miranda, A. Pajares, A. Lemos, J.M.F. Ferreira.** 1, 2014, Journal of the European Ceramic Society, Vol. 34, p. 107-118.

33. *Biology of Bone Tissue: Structure, Function, and Factors That Influence Bone Cells.* **Rinaldo Florencio-Silva, Gisela Rodrigues da Silva Sasso, Estela Sasso-Cerri, Manuel Jesus Simões, Paulo Sérgio Cerri.** 2015, 2015, BioMed Research International.

34. **Qizhi Z. Chen, Ian D. Thompson, Aldo R. Boccaccini.** 45S5 Bioglasss-derived glass–ceramic scaffolds for bone tissue engineering. *Biomaterials.* 2006, 27.

35. **P.Rokkanena, .S.Vainionpää, P.Törmälä, J.Kilpikari, O.Böstman, K.Vihtonen, J.Laiho, M.Tamminmäki.** BIODEGRADABLE IMPLANTS IN FRACTURE FIXATION: EARLY RESULTS OF TREATMENT OF FRACTURES OF THE ANKLE. *The Lancet.* 1985, Vol. 325, 8443.

36. **Oscar Peitl Filho, Guy P. La Torre, L. L. Hench.** Effect of crystallization on apatite-layer formation of bioactive glass 45S5. *Journal of Biomedical Materials Research.* 1996, Vol. 30, 4.

37. **Nerem, Robert M.** Chapter 2 - The Challenge of Imitating Nature. *Principles of Tissue Engineering.* s.l. : Elsevier, 2000, p. 9-15.

38. *Stiffness of compact bone: Effects of porosity and density.* **Mitchell B. Schaffler, David B. Burr.** 1, s.l. : Journal of Biomechanics, 1988, Vol. 21. 10.1016/0021-9290(88)90186-8.

39. **McIntire, Charles W. Patrick Jr.Antonios G. MikosLarry V.** Chapter I – Prospectus of Tissue Engineering. *Frontiers in Tissue Engineering.* s.l. : Elsevier, 1998, p. 3-11.

40. **Martin Meischel, Daniel Hörmann, Johannes Draxler, Elmar K. Tschegg, Johannes Eichler, Thomas Prohaska, Stefanie E. Stanzl-Tschegg.** Bone-implant degradation and mechanical response of bone surrounding Mg-alloy implants. *Journal of the Mechanical Behavior of Biomedical Materials.* 2017, 17.

41. *Bone Grafting and Guided Bone Regeneration for Immediate Dental Implants in Humans.* **Marlin E. Gher, George Quintero, Daniel Assad, Edward Monaco and A. C. Richardson.** 9, 1994, Journal of Periodontology, Vol. 65, p. 881-891.

42. *Reaction kinetics of bioactive ceramics, part IV: Effect of glass and solution composition.* **LaTorre, L. L. Hench and G. P.** 5, Kyoto : Kobonshi Kankokai, Inc., 1992.

43. **Larry L. Hench, Delbert E. Day, Wolfram Ho¨land and Volker M. Rheinberger.** Glass and Medicine. *International Journal of Applied Glass Science.* 2010, 1.

44. **Lakshmi, Vidya Krishnan and T.** Bioglass: A novel biocompatible innovation. *J Adv Pharm Technol Res.* 2013, Vol. 2, 4.

45. **Kansal I, Reddy A, Muñoz F, Choi SJ, Kim HW, Tulyaganov DU, Ferreira JM.** Structure, biodegradation behavior and cytotoxicity of alkali-containing alkaline-earth phosphosilicate glasses. *Materials Science & Engineering C, Materials for Biological Applications.* 2014, 44.

46. *Biodegradable and bioactive porous polymer/inorganic composite.* **K. Rezwan, Q.Z. Chen, J.J. Blaker, Aldo Roberto Boccaccini.** 27, 2006, Biomaterials, p. 3413-3431.

47. **Jones, Julian R.** Review of bioactive glass: From Hench to hybrids. *Acta Biomaterialia.* 2013, Vol. 9, 1.

48. *Control of the viscous behavior of highly concentrated mullite suspension for robocasting.* **John N. Stuecker, Joseph Cesarano III, Deidre A. Hirschfeld.** 42, 2003.

49. **James M. Pachence, Joachim Kohn.** Chapter 22 - Biodegradable Polymers. *Principles of Tissue Engineering.* s.l. : Elsevier, 2000, p. 263-277.

50. —. Chapter 22 - Biodegradable Polymers. *Principles of Tissue Engineering.* s.l. : Elsevier, 2000, p. 263-277.

51. *Is there scientific evidence favoring the substitution of commercially pure titanium with titanium alloys for the manufacture of dental implants?* **Jairo M. Cordeiro, Valentim A.R. Barão.** 71, 2017, Materials Science and Engineering, p. 1201-1215.

52. **J. Cesarano, Baer, Calvert.** Proceedings of the Solid Freeform Fabrication Symposium. Austin, TX : s.n., 1997, Vol. 542, p. 25-32.

53. **Ishu Kansal, Ashutosh Goel, Dilshat U. Tulyaganov, Maria J. Pascual, Hye-Young Lee, Hae-Won Kime.** Diopside (CaO$MgO$2SiO2)–fluorapatite (9CaO$3P2O5$CaF2) glass ceramics: potential materials for bone tissue engineering. *Journal of Dynamic Article Links.* 2011, 21.

54. **Ippokratis Pountos, Theodora Georgouli, Giorgio M. Calori, and Peter V. Giannoudis.** Do Nonsteroidal Anti-Inflammatory Drugs Affect Bone Healing? *The Scientific World Journal.* 2012.

55. *Ionic Products of Bioactive Glass Dissolution Increase Proliferation of Human Osteoblasts and Induce Insulin-like Growth Factor II mRNA Expression and Protein*

*Synthesis.* **I. D. Xynos, A. J. Edgar, L. D. K. Buttery, L. L. Hench, J. M. Polak.** 276, 2000, Biochemical and Biophysical Reasearch Communications, p. 461-465.

56. **Erica Pensini, Christopher M. Yip, Denis O'Carroll, Brent E. Sleep.** Carboxymethyl cellulose binding to mineral substrates: Characterization by atomic force microscopy–based Force spectroscopy and quartz-crystal microbalance with dissipation monitoring. *Journal of Colloid and Interface Science.* 2013, 402.

57. *Analysis of Bone Tissue Mechanical Properties.* **Diana Milcic, Jadranka Keros and Andrija Bosnjak.** 27, s.l. : Original scientific Paper, 2003, Vol. 2. UDC 572.781:612.753.

58. **Daniel C. Clupper, John J. Mecholsky Jr, Guy P. LaTorre, David C. Greenspan.** Bioactivity of tape cast and sintered bioactive glass-ceramic. *Biomaterials.* 2002, 23.

59. **D.C. Clupper, L.L. Hench.** Crystallization kinetics of tape cast bioactive glass 45S5. *Journal of Non-Crystaline Solids.* 2003, 318.

60. *An Overview of The Effects of Thermal Processing on Bioactive Glasses.* **D. Bellucci, V. Cannillo, A. Sola.** 42, 2010, Science of Sintering, p. 307-320.

61. **Cortez PP, Brito AF, Kapoor S, Correia AF, Atayde LM, Dias-Pereira P, Afonso A, Goel A, Ferreira JMF.** The in vivo performance of an alkali-free bioactive glass for bone grafting, FastOs V R BG, assessed with an ovine model. *Journal of Biomedical Materials Research Part B Applied Biomaterials.* 2015.

62. **Bohner, Marc.** Silicon-substituted calcium phosphates – A critical view. *Biomaterials.* 2009, Vol. 30, 32.

63. **Bankoff, Antonia Dalla Pria.** Biomechanical Characteristics of the Bone. [aut. libro] Dr. Tarun Goswami. *Human Musculoskeletal Biomechanics.* Shangai : InTech, 2012.

64. **Ammam, Malika.** Electrophoretic deposition under modulated electric fields: a review. *RSC Advances.* 2012, 2.

65. *Computational wear prediction of artificial knee joints based on a new wear.* **Abdellatif Abdelgaied, Feng Liu, Claire Brockett, Louise Jennings, John Fisher, Zhongmin Jin.** 44, 2011, Journal of Biomechanics, p. 1108-1116.

66. **A. Gama Goicochea, M.A. Balderas Altamirano, R. Lopez-Esparza, M. A. Waldo, E. Perez.** ON THE COMPUTATIONAL MODELING OF THE VISCOSITY

OFCOLLOIDAL DISPERSIONS AND ITS RELATION WITH BASIC MOLECULAR INTERACTIONS. *European Journal of Physics.* 2015.

67. **A. Carradò, F. Perrin-Schmitt, Q.V. Le, M. Giraudel, C. Fischer, G. Koenig, L. Jacomine, L. Behr, A. Chalom, L. Fiette, A. Morlet, G. Pourroy.** Nanoporous hydroxyapatite/sodium titanate bilayer on titanium implants for improved osteointegration. [Online] 13 January 2017. http://dx.doi.org/10.1016/j.dental.2016.12.013.

68. **[Online] http://www.lightinghomes.net/gallery/four-components-of-skeletal-system.html.**